Geophysical Modeling in VLBI

Dan MacMillan
NVI Inc./NASA GSFC

EGU and IVS Training School on VLBI for Geodesy and Astrometry
Aalto University, Espoo, Finland

March 2-5, 2013

Overview

1. Calculation of the Theoretical Delay

2. Tide Generating Potential

3. Site Displacement Contributions to the Calculation of Theoretical Delay

    a. Solid Earth Tides

    b. Rotational Deformation due to Polar Motion (Pole Tide)

    c. Ocean Pole Tide Loading

    d. Ocean Tidal Loading

    e. Nontidal Loading (Atmosphere, Hydrology, Ocean)

    f. Other Models (antenna thermal deformation)

Theoretical Delay

The theoretical delay is calculated by programs like CALC (input to SOLVE)

There are several steps that are involved in this procedure:

Step 1: Transformation of positions in crust-fixed terrestrial reference frame (TRF) to geocentric celestial reference system (J2000)

$$Q = PNUXY$$

Precession/Nutation x Spin x Polar Motion

$$\vec{r}_c = Q\vec{r}_t$$

Earth Orientation Parameters (EOP)

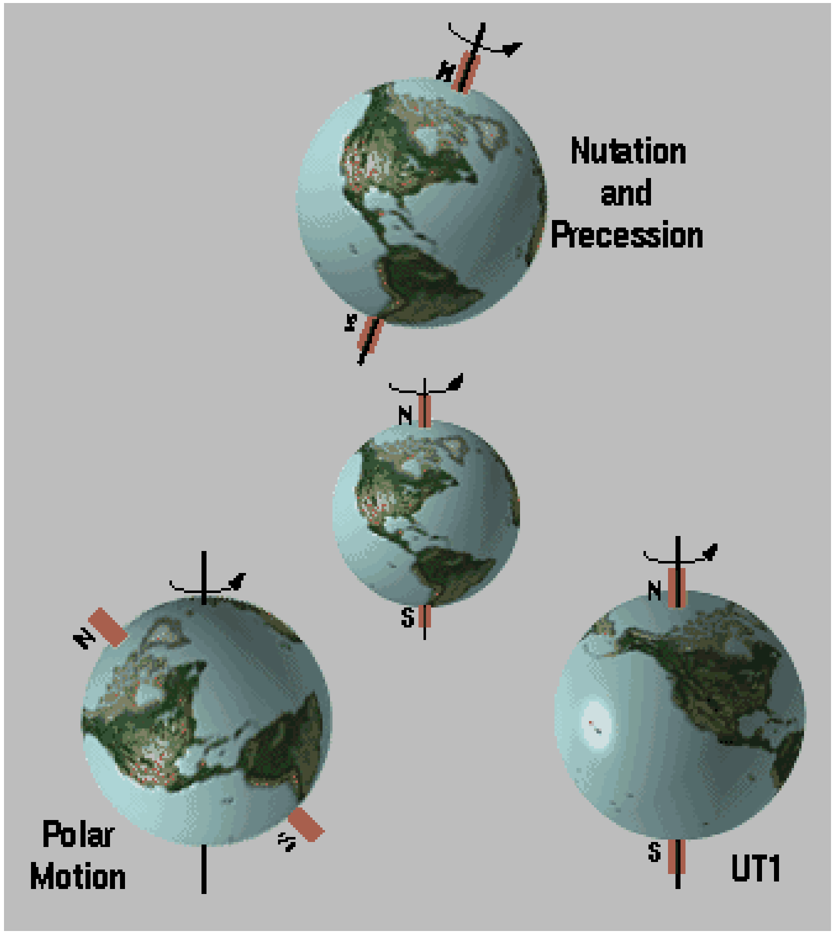

Nutation/precession: periodic and long-term motion of the spin axis relative to CRF

Polar motion: motion of the geographic pole relative to the spin axis

UT1: describes the non uniform daily rotation of the Earth

Theoretical Delay

Step 2. Compute Displacement Models and Delay Corrections for each site

- Solid Earth (largest for 12 h band, up to 40 cm in vertical)
- Ocean Loading (largest for 12 h band, mm-cm in vertical)
- Pole Tide (12,14 months period, mm-cm)
- Ocean Pole Tide Loading (mm)
- [Atmosphere Pressure Loading] –{in Solve}
- Site velocities – {in Solve}

Other Physical Offsets:

- Axis offset correction (cm-m)
- [Antenna thermal expansion/contraction (mm-cm)] –{in Solve}

Refractive Media Delays:

- Atmosphere delays (NMF) (nsecs) –{VMF in Solve}
- [Ionosphere delays] (hundreds of psec) {X/S or GPS in Solve}

Causes of Site Motion and Variations in Earth Orientation

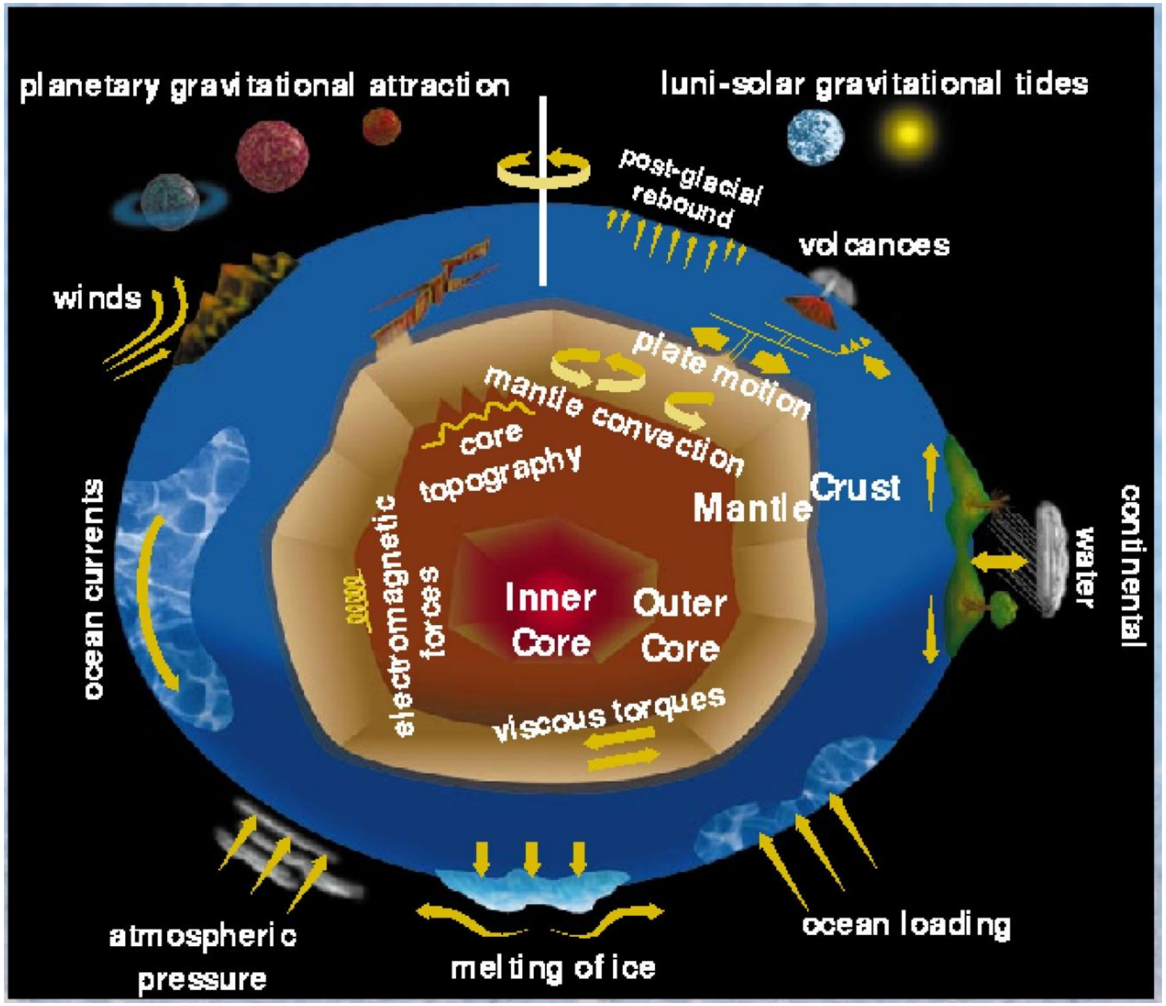

Plate Motion

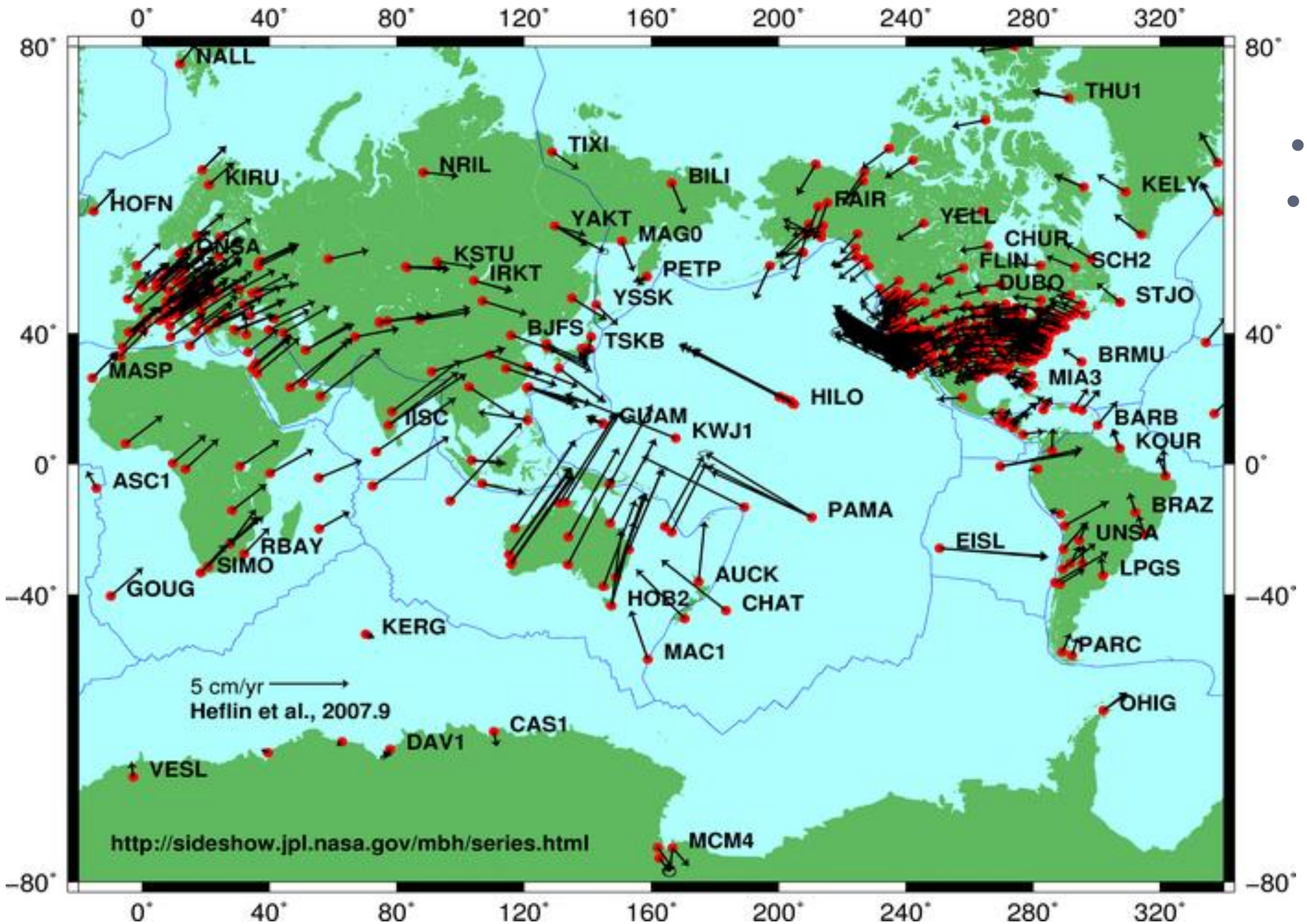

- GPS velocities
- Plate rotation poles

Theoretical Delay

Step 3. Apply displacements from Step 2 to station positions in J2000.0 and compute baseline vector $\vec{b} = \vec{r}_{c2} - \vec{r}_{c1}$

Compute quasar source unit vector, s, pointing in the source direction

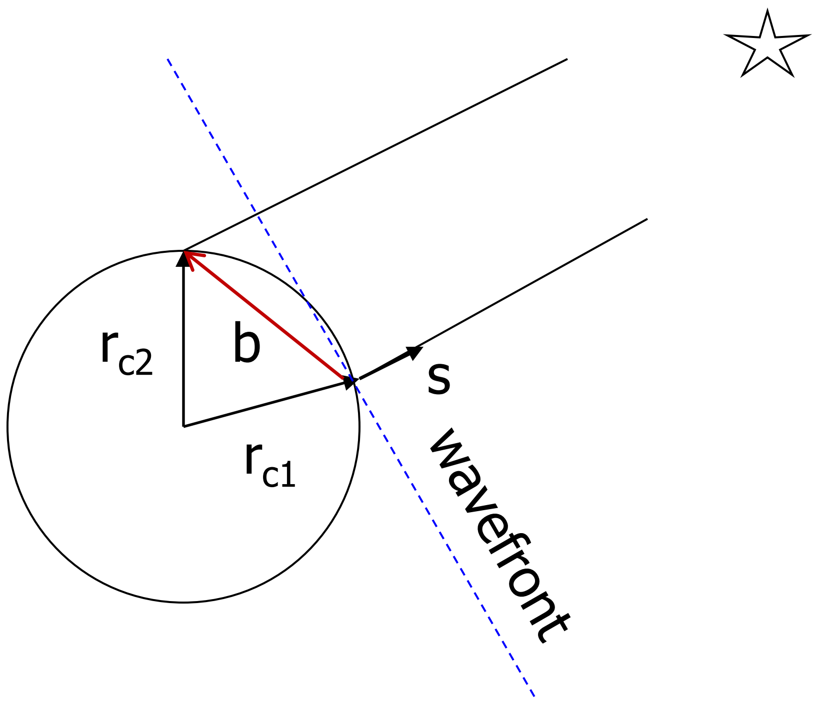

$$\tau \approx -\vec{b} \cdot \hat{s}$$

Theoretical Delay

Step 4. Compute Theoretical Delay

- Use the Eubanks 'Consensus' Model.
  [see IERS Conventions 2010]

- acccount for gravitational deflection from sun, moon, Earth, other planets.

- Requires relativistic transformation to/from solar system barycentric coordinates

- Add atmosphere geometric path delay contribution

Theoretical Delay (Consensus Model)

Compute gravitational delays for each gravitating body

$$\Delta T_g = \sum_J \Delta T_{gJ}$$ Sun + planets + Earth

Bending delay includes effect of 1) motion of gravitating body during propagation, 2) motion of station 2 during propagation, 3) component of light travel time between gravitating body and site 1 in source direction K.

Station coordinates in the barycentric frame from coordinates $x_i(t_1)$ in GCRS frame

$$X_i(t_1) = X_{\oplus}(t_1) + x_i(t_1)$$

Coordinates of the geocenter in the barycentric frame

Vacuum delay in the solar system barycentric (SSB) frame

$$T_2 - T_1 = -\frac{1}{c} K \cdot [X_2(T_2) - X_1(T_1)] + \Delta T_g$$

Source vector in SSB frame

Consensus Model

Convert barycentric vacuum delay to geocentric vacuum delay by applying Lorentz transformation

$$t_{v2} - t_{v1} = \frac{\Delta T_g - \frac{K \cdot b}{c}\left[1 - \frac{(1+\gamma)U}{c^2} - \frac{|V_\oplus|^2}{2c^2} - \frac{V_\oplus \cdot w_2}{c^2}\right] - \frac{V_\oplus \cdot b}{c^2}(1 + K \cdot V_\oplus / 2c)}{1 + \frac{K \cdot (V_\oplus + w_2)}{c}}$$

Baseline vector: $b = x_2(t_1) - x_1(t_1)$

Barycentric velocity of the geocenter: $V_\oplus$

Geocentric velocity of site 2: w_2

Gravitational potential energy at the geocenter due to the sun's mass: U

PPN parameter: γ (Parametrized Post Newtonian) γ =1 for general relativity

Adding the troposphere geometric path delay contribution -> total delay

Tide Generating Potential

Tidal Potential due to an external body (moon, Sun, planet)

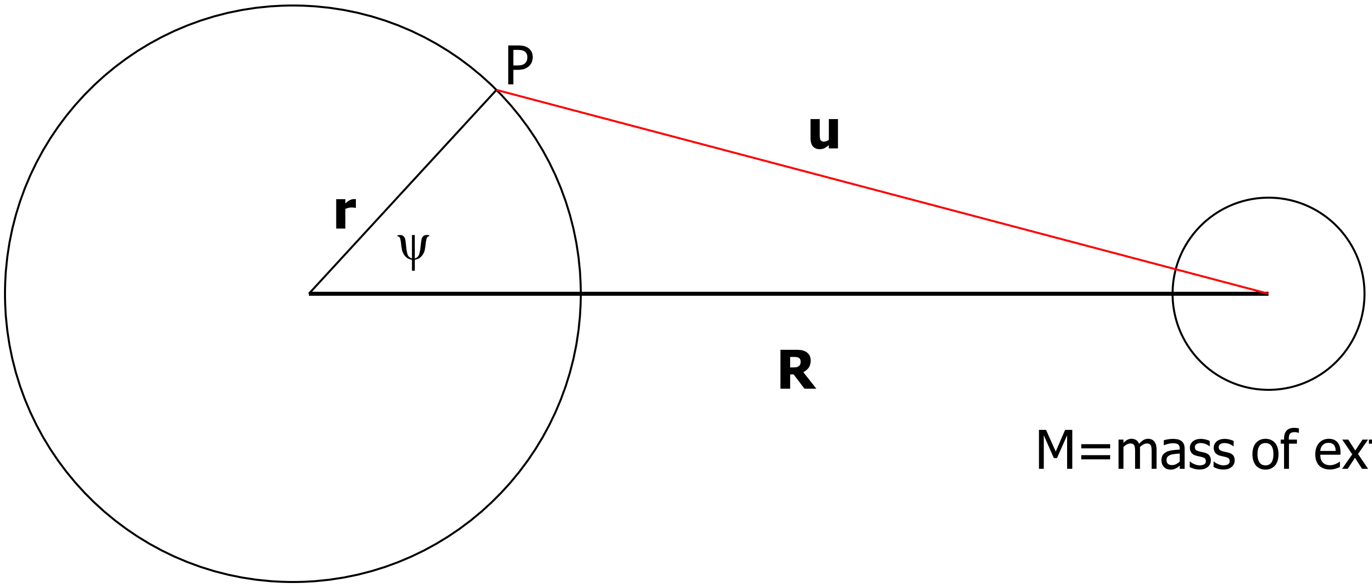

M=mass of external body

$$W = GM\left(\frac{1}{u} - \frac{1}{R} - \frac{r\cos\psi}{R^2}\right)$$

Use the reciprocal distance expression for 1/u

$$W = \frac{GM}{R}\sum_{n=2}^{\infty}\left(\frac{r}{R}\right)^n P_n(\cos\psi)$$

Tide Generating Potential

Main Tidal Potential:

$$W_2 = \frac{GM}{R}\left(\frac{r}{R}\right)^2 P_2(\cos\psi)$$

$$a_r = G\frac{Mr}{2R^3}(1+3\cos(2\psi))$$

$$a_\psi = -G\frac{Mr}{2R^3}3\sin(2\psi)$$

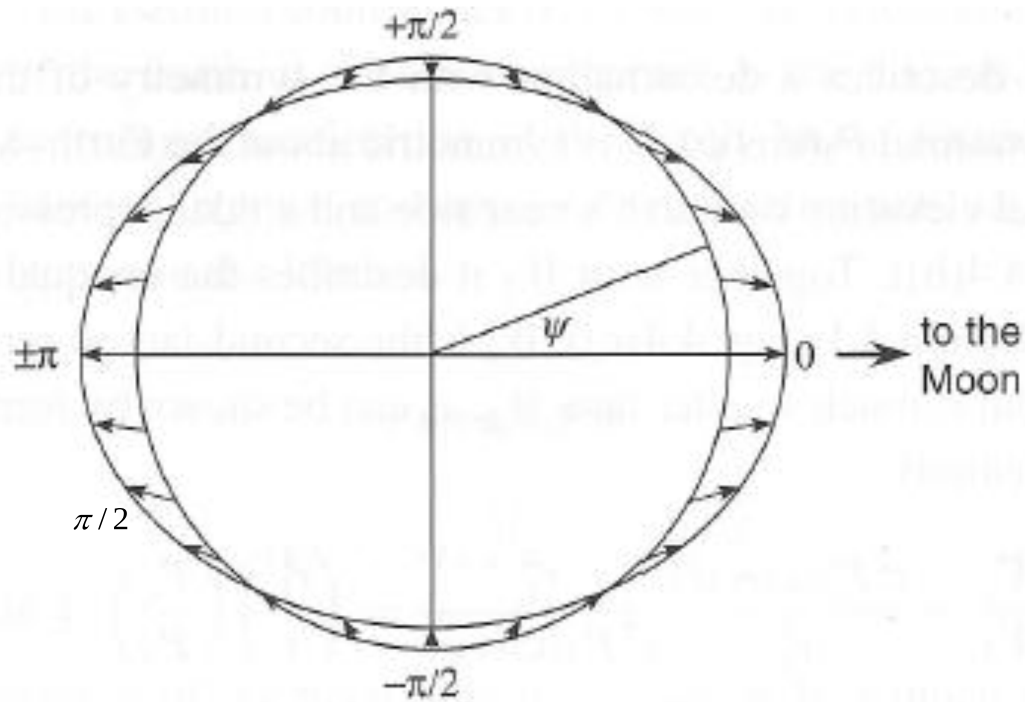

Direction of lunar tidal-raising force:

Only radial component at multiples of $\pi/2$

Transverse+radial at intermediate points

Tide Generating Potential

Third-degree Potential:

$$W_3 = \frac{GM}{R}\left(\frac{r}{R}\right)^3 P_3(\cos\psi)$$

$$\frac{W_2}{W_3} = \left(\frac{R}{r}\right)\left(\frac{P_2}{P_3}\right) \geq 80$$

Relative strength of the lunar and solar tide-raising forces

$$\frac{a_L}{a_S} = \frac{M_{moon}}{M_{sun}}\left(\frac{R_{sun}}{R_{moon}}\right)^3 \approx 2.2$$

Tide Generating Potential

Hartmann and Wenzel (1995) expand the TGP in terms of the Legendre functions of the ephemerides

$$V(t) = GM_b \sum_{n=2}^{\infty} \sum_{m=0}^{n} \frac{r^n}{r_b^{n+1}} \frac{1}{2n+1} P_{nm}(\cos\theta) P_{nm}(\cos\Theta_b(t)) \times \cos[(m(\lambda - \Lambda_b(t))]$$

+ terms that account for the Earth's flattening effect

(θ, λ, r) are the geocentric station coordinates

Evaluate the potential using geocentric coordinates

$[\Theta_b(t), \Lambda_b(t)]$ of the (sun,moon,planets)

Hartmann and Wenzel used JPL ephemerides DE200/LE200

Tide Generating Potential

The full tidal potential was expressed by HW in terms of the following expansion by process of least-squares fitting and spectral analysis of residuals:

$$V(t)=\sum_{n=1}^{6}\sum_{m=0}^{n}\left(\frac{r}{a}\right)^{n}\overline{P}_{nm}(\cos\theta)\times$$

$$\times\sum_{i}\left[C_i^{nm}(t)\cos(\alpha_i(t))+S_i^{nm}(t)\sin(\alpha_i(t))\right]$$

$$C_i^{nm}=C0_i^{nm}+t\cdot C1_i^{nm}$$

$$S_i^{nm}=S0_i^{nm}+t\cdot S1_i^{nm}$$

Truncated at n=6 (moon), n=3 (sun), n=2 (planets)

Estimated 12935 coefficients

Functions of the astronomical arguments for each tide:

$$\alpha_i(t)=m\cdot\lambda+\sum_{j=1}^{j=11}k_{ij}\cdot\xi_j(t)$$

$$\tau=mean\_local\_lunar\_time$$

$$s=mean\_lunar\_longitude$$

$$h=mean\_solar\_longitude$$

$$p=mean\_longitude\_lunar\_perigee$$

$etc.$

Table 1. Maximum tidal potential and gravity tide due to the Moon and the Sun.

body	ℓ	$V_{(t)}$ [m^2/s^2]	$\partial V_{(t)}/\partial r$ [pm/s^2]
Moon	2	4.41	1 381 512.42
Moon	3	$7.88\cdot10^{-2}$	37 085.33
Moon	4	$1.41\cdot10^{-3}$	884.91
Moon	5	$2.53\cdot10^{-5}$	19.80
Moon	6	$4.52\cdot10^{-7}$	0.43
Moon	7	$8.09\cdot10^{-9}$	< 0.01
Moon	$J_2^{\oplus}$	$5.12\cdot10^{-4}$	80.30
Sun	2	1.60	501 604.61
Sun	3	$6.80\cdot10^{-5}$	31.99
Sun	4	$2.89\cdot10^{-9}$	< 0.01
Sun	$J_2^{\oplus}$	$4.42\cdot10^{-7}$	0.07

Tide Generating Potential

Tab. 3.1. Principal Gravimetric Partial Tides for $\overline{\varphi} = 45°$, $h = 0$

symbol	name	period (solar hours)	amplitude $\left(\mathrm{nm\,s^{-2}}\right)$
long-periodic waves			
M0	const. *l* tide	∞	102.9
S0	const. *s* tide	∞	47.7
Ssa	declin. tide to S0	182.62 d	14.8
Mm	ellipt. tide to M0	27.55 d	16.8
Mf	declin. tide to M0	13.66 d	31.9
diurnal waves			
O1	main diurnal *l* tide	25.82 h	310.6
P1	main diurnal *s* tide	24.07 h	144.6
Q1	ellipt. tide to O1	26.87 h	59.5
K1	main diurnal *ls* decl. tide	23.93 h	436.9
semi-diurnal waves			
M2	main *l* tide	12.42 h	375.6
S2	main *s* tide	12.00 h	174.8
N2	ellipt. tide to M2	12.66 h	71.9
K2	declin. tide to M2, S2	11.97 h	47.5
ter-diurnal waves			
M3	terdiurn. *l* tide	8.28 h	5.2

Solid Earth Tides

First compute in-phase displacements in the time domain, here for deg 2, but deg 3 is similar.

- nominal (frequency independent) values for Love numbers (h_n, l_n)
- avoids having to sum over very large number of terms of TGP above

$$V(r,R) = \frac{GM}{R}\sum_{n=2}^{\infty}\left(\frac{r}{R}\right)^n P_n(\cos\Theta)$$

Love number response

$$\Delta_n(u,e,n) = \frac{1}{g}[h_n V_n \hat{r}, \frac{l_n}{\cos\phi}\frac{\partial V_n}{\partial\lambda}\hat{e}, l_n\frac{\partial V_n}{\partial\phi}\hat{n}]$$

deg	Moon	Sun
2	425 mm	173 mm
3	7.5 mm	0.008 mm
4	0.13 mm	0.000 mm

$$\Delta\vec{r}_n = \frac{M}{M_E} r\left(\frac{r}{R}\right)^{n+1}[h_n P_n(\cos\Theta)\hat{r} + l_n P_n'(\Theta)\{\hat{R} - \cos\Theta\hat{r}\}]$$

$$\cos\Theta = \hat{R}\cdot\hat{r}$$

$$F_j = \frac{GM_j R_E^4}{GM_E R_j^3}$$

Displacement from degree 2 TGP with nominal values for h2 and l2

$$\Delta\vec{r}_2 = \sum_{j=2}^{3} F_j\{\bar{h}_2\hat{r}[\frac{3}{2}(\hat{R}_j\cdot\hat{r})^2 - \frac{1}{2}] + 3\bar{l}_2(\hat{R}_j\cdot\hat{r})[\hat{R}_j - (\hat{R}_j\cdot\hat{r})\hat{r}]\}$$

$\vec{R}_j$ -Vector from geocenter to moon(j=2) or sun(j=3)

R_E -Earth radius

Solid Earth Tides

Other Contributions to Solid Earth Tides

- Necessary to reach the targeted accuracy better than 1 mm

- Requires additional correction terms to the in-phase terms described above:

  1) Out-of-phase correction arising from imaginary part of Love numbers, which models the anelastic component of deformation

  Anelastic deformation => earth response lags the time variation of the potential

  2) Frequency domain corrections

  - in-phase correction for degree-2 in the diurnal and long-period bands
  - out-of-phase correction for degree-2 long-period band

Rotational Deformation due to Polar Motion - Poletide

$$\vec{a} = \vec{a}' + 2\vec{\Omega}\times\vec{v}' + \vec{\Omega}\times(\vec{\Omega}\times\vec{r}')$$

Acceleration in the fixed frame, where the primed system is rotating

Coriolis acceleration   Centrifugal acceleration

$$\vec{a}_c = \vec{\Omega}\times(\vec{\Omega}\times\vec{r}) = \vec{\Omega}(\vec{r}\cdot\vec{\Omega}) - \Omega^2\vec{r}$$

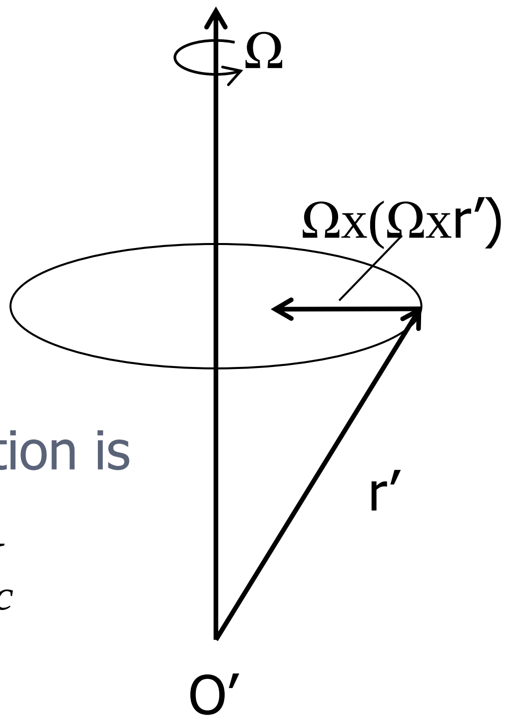

The centrifugal potential corresponding to this acceleration is

$$V_c = \frac{1}{2}[\Omega^2 r^2 - (\vec{\Omega}\cdot\vec{r})^2] = \frac{1}{2}|\vec{\Omega}\times\vec{r}|^2$$

$$\vec{a}_c = -\nabla V_c$$

Rotational Deformation due to Polar Motion - Poletide

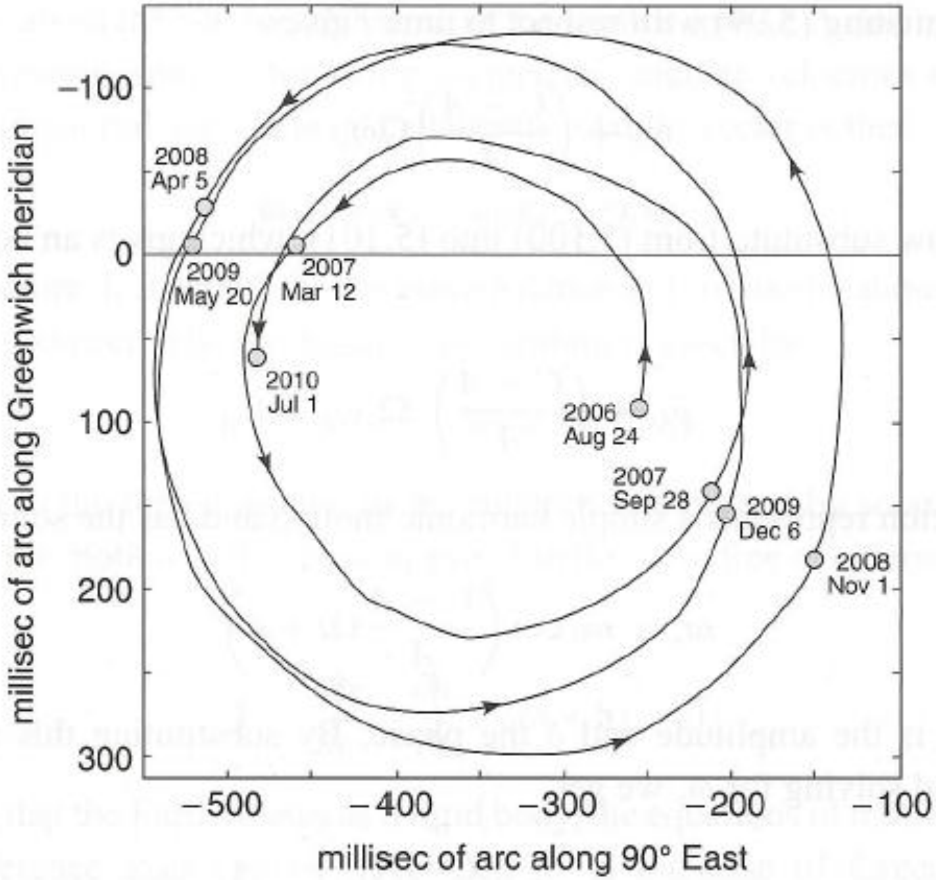

Fig. 5.8. The instantaneous rotation axis of the Earth exhibits a nearly circular motion with period 435 days – the Chandler wobble – and an annual circular motion. These motions are superposed on a slow drift of about 20 m per century along longitude 80 °W. Data source: International Earth Rotation and Reference Systems Service.

Motion of the rotation axis about the geographic pole: Radius ~ 10-12m

Rotational Deformation due to Polar Motion - Poletide

$$V = \frac{1}{2}[\Omega^2 r^2 - (\vec{\Omega}\cdot\vec{r})^2] = \frac{1}{2}|\vec{\Omega}\times\vec{r}|^2$$

Angular rotation of the Earth

$$\vec{\Omega} = \Omega_0[m_x\hat{x} + m_y\hat{y} + (1+m_z)\hat{z}]$$

Average rotation rate

Time-dependent offsets of pole

Fractional variation in rotation rate

$$V = \frac{1}{2}\Omega_0^2[x^2 + y^2 + (x^2+y^2)2m_z - 2z(m_x x + m_y y)] + O(m^2)$$

[Wahr, 1985]

m_z variation ~ 1/100 m_x or m_y

$$V(\theta,\lambda) = -\frac{1}{2}\Omega_0^2 r^2[\sin 2\theta(m_x\cos\lambda + m_y\sin\lambda)]$$

Site displacement response to the potential via Love numbers:

$$\Delta U = \frac{h_2}{g}V \qquad \Delta E = \frac{l_2}{g}\frac{1}{\sin\theta}\frac{\partial}{\partial\lambda}V \qquad \Delta N = \frac{l_2}{g}\frac{\partial}{\partial\theta}V \qquad h_2 = 0.6207, l_2 = 0.0836$$

Rotational Deformation due to Polar Motion - Poletide

$$\Delta U = -33 \sin 2\theta (m_x \cos\lambda + m_y \sin\lambda)$$

$$\Delta E = 9 \cos\theta (m_x \sin\lambda - m_y \cos\lambda)$$

in mm

$$\Delta N = -9 \cos 2\theta (m_x \cos\lambda + m_y \sin\lambda)$$

Mean pole $(\bar{x}_p, \bar{y}_p)$

IERS Conventions (2010): quadratic before 2010, linear after 2010

$$m_x = x_p - \bar{x}_p \qquad m_y = y_p - \bar{y}_p$$

Ocean Pole Tide Loading

What is the effect of the centrifugal potential on the ocean mass?

Additional potential due to external potential V
$U = k V$

$H1 = (1+k)V/g$ Ocean surface (geoid) adjusts to this level.

Height of the body tide. Deformation adjustment of solid earth height

$H2 = h V/g$

Resultant height of the ocean (measured relative to deformed solid earth)

$H = H1-H2 = (1+k-h)V/g$

k and h are Love numbers that give response from the external potential

Ocean Pole Tide Loading

$$V(\theta,\lambda) = -\frac{1}{2}\Omega_0^2 r^2[\sin 2\theta(m_x \cos\lambda + m_y \sin\lambda)]$$

Change in the ocean height due to external (centrifugal) potential V:

$$\eta = (1+k-h)\frac{V(\theta,\lambda)}{g}$$

Compute the site loading effect by convolving with loading Green's function

$$\Delta u(\theta,\lambda,t) = \int_{ocean} G(\theta,\lambda;\theta',\lambda')\rho_{seawater}[\eta(\theta',\lambda',t) - \overline{\eta}(t)]d\Omega'$$

Subtract the average ocean height at each epoch
=> ocean mass conservation

Ocean Pole Tide Loading

Centrifugal effect of polar motion => Redistribution of ocean mass => Change in loading mass => site position displacement

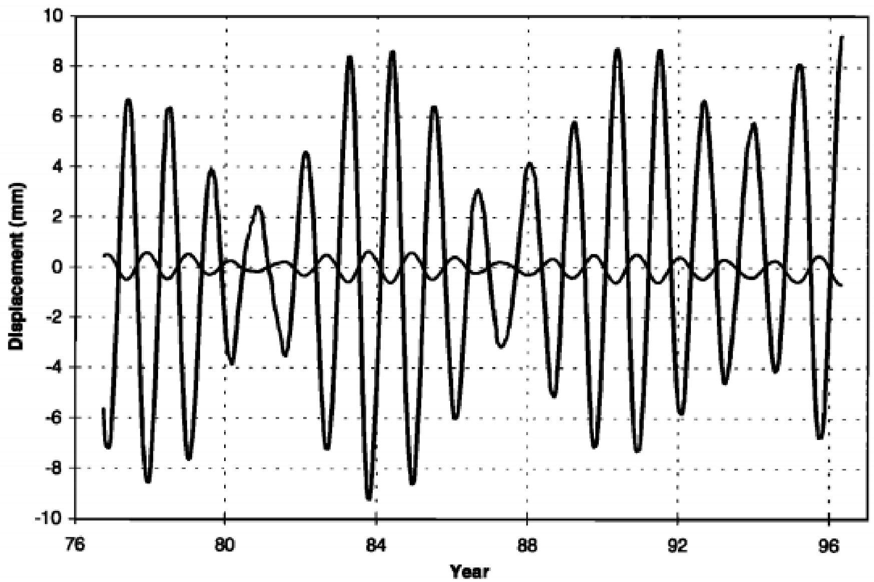

Figure 4. Up displacement at Haystack due to EOP variations. The larger-amplitude curve shows the direct effect of the pole tide. The smaller-amplitude curve shows the effect of polar motion induced ocean loading.

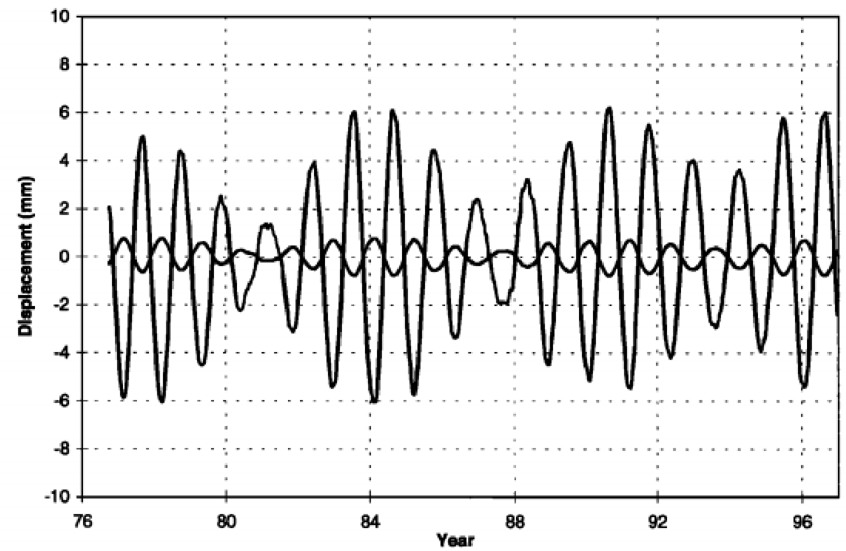

Figure 5. Up displacement at Kauai due to EOP variations. The larger-amplitude curve the direct effect of the pole tide. The smaller-amplitude curve shows the effect of polar motion induced ocean loading.

(Plots from Gipson and Ma, 1998)

- Pole tide effect is much larger than the polar motion induced loading
- The effects are 180 deg out of phase
- See S. D. Desai (2002) for version of model in IERS Conventions

Ocean Loading Tides

Ocean Tide Models

Model code	Reference	Input	Resolution
Schwiderski	Schwiderski (1980)	Tide gauge	$1° \times 1°$
CSR3.0, CSR4.0	Eanes (1994)	TOPEX/Poseidon altim.	$1° \times 1°$
	Eanes and Bettadpur (1995)	T/P + Le Provost loading	$0.5° \times 0.5°$
TPXO5	Egbert *et al.* (1994)	inverse hydrodyn. solution from T/P altim.	256×512
TPXO6.2	Egbert *et al.* (2002), see <[3]>	idem	$0.25° \times 0.25°$
TPXO7.0, TPXO7.1	idem	idem	idem
FES94.1	Le Provost *et al.* (1994)	numerical model	$0.5° \times 0.5°$
FES95.2	Le Provost *et al.* (1998)	num. model + assim. altim.	$0.5° \times 0.5°$
FES98	Lefèvre *et al.* (2000)	num. model + assim. tide gauges	$0.25° \times 0.25°$
FES99	Lefèvre *et al.* (2002)	numerical model + assim. tide gauges and altim.	$0.25° \times 0.25°$
FES2004	Letellier (2004)	numerical model	$0.125° \times 0.125°$
GOT99.2b, GOT00.2	Ray (1999)	T/P	$0.5° \times 0.5°$
GOT4.7	idem	idem	idem
EOT08a	Savcenko *et al.* (2008)	Multi-mission altimetry	$0.125° \times 0.125°$
AG06a	Andersen (2006)	Multi-mission altimetry	$0.5° \times 0.5°$
NAO.99b	Matsumoto *et al.* (2000)	num. + T/P assim.	$0.5° \times 0.5°$

Ocean Loading Tides

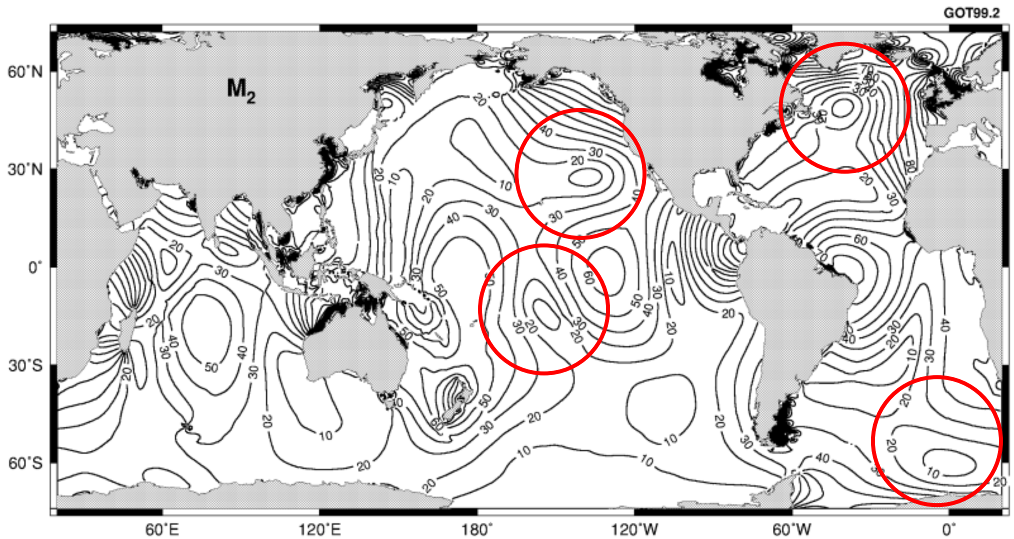

Figure A11. Amplitude of M_2 tide. Contour interval = 10 cm.

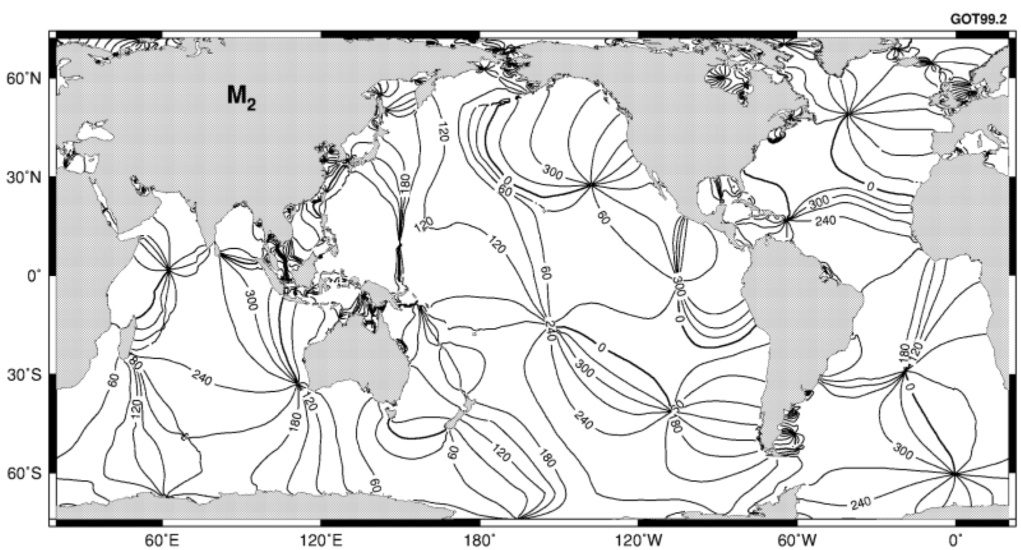

Figure A12. Greenwich phase lag of M_2 tide. Contour interval = 30°.

- Plots show lines of constant amplitude or phase
- Phase angles are with respect to the Greenwich meridian.
- Areas of zero amplitude are 'amphidromes' - points about which the tide rotates (here with ~12h M2 tidal period)

M2 semi-diurnal tide

GOT99.2 model (R. Ray) based on Topex altimeter + hydrodynamic model FES94.1

Ocean Loading Tides

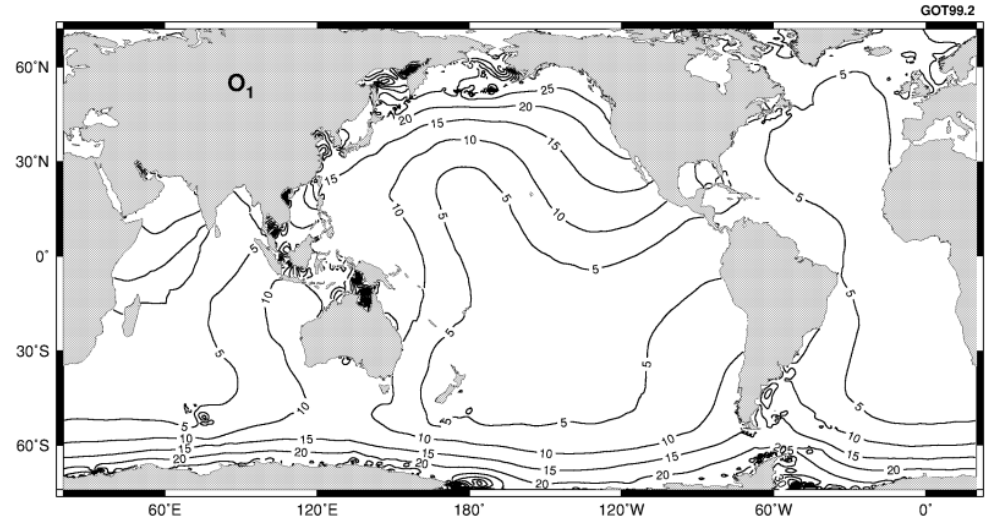

Figure A3. Amplitude of O_1 tide. Contour interval = 5 cm.

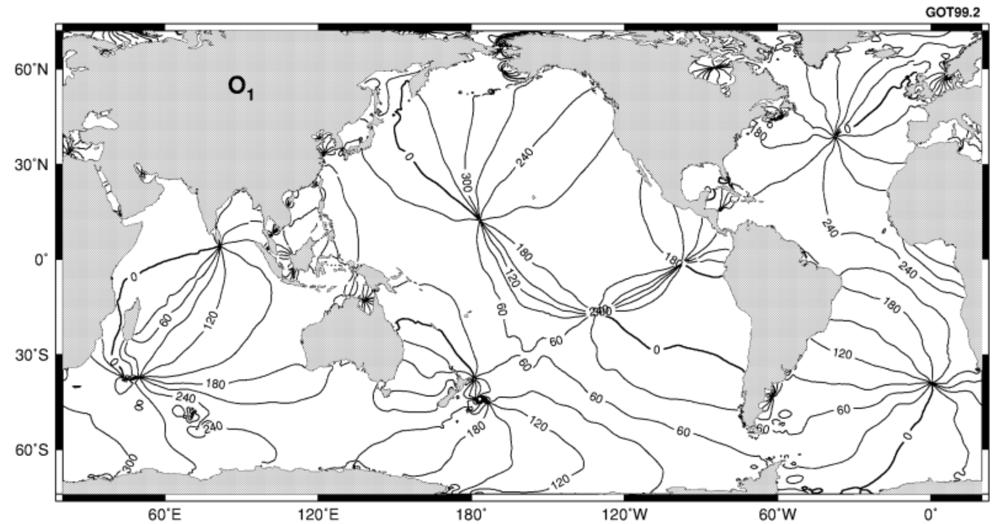

Figure A4. Greenwich phase lag of O_1 tide. Contour interval = 30°.

O1 diurnal tide

GOT99.2 model

Ocean Tidal Loading

Computation of ocean tidal loading

- Tide elevation from global tide maps, where Z and δ are the amplitudes and phases of each specific partial tides k at (ϕ,λ)

$$\xi(k,\phi,\lambda,t) = Z_k(\phi,\lambda)\cos[\omega_k t + \chi_k - \delta_k(\phi,\lambda)]$$

- Response of oceans to the Tide Generating Potential is much different than for solid earth

- Response depends strongly on local/regional conditions

- Loading at a site has to be computed by globally integrating the loading Green's function over the tide elevation mass for each tidal constituent

Ocean Tidal Loading

Site displacement due to loading is given by a sum over tides

$$x_k(t) = \sum_{j=1}^{11} A_{kj} \cos(\chi_j(t) - \Phi_{kj}), (k = U, E, N)$$

The astronomical argument of the tide

For each partial ocean tide, the tide crest occurs Φkj hours after the crest of the solid earth tide at the Greenwich meridian.

1) Loading UEN amp/phase are computed for 11 main tides (M2,S2,N2,K2,K1,O1,P1,Q1,Mf,Mm,Ssa) e.g., at Scherneck website

2) Better to also use HARDISP routine that computes loading based on 342 constituents found by interpolating tidal admittances based on the 11 main tides. (Error too large if keep only the 11 tide contribution) See IERS 2010 Conventions.

Ocean Loading Tides

Table 7.5: Sample of an ocean loading table file in BLQ format. Each site record shows a header with information on the ocean tide model and the site name and geographic coordinates. First three rows of numbers designate amplitudes (meter), radial, west, south, followed by three lines with the corresponding phase values (degrees).

Columns designate partial tides $M_2, S_2, N_2, K_2, K_1, O_1, P_1, Q_1, M_f, M_m$, and S_{sa}.

```
$$
  ONSALA
$$ CSR4.0_f_PP ID: 2009-06-25 20:02:03
$$ Computed by OLMPP by H G Scherneck, Onsala Space Observatory, 2009
$$ Onsala,                                  lon/lat: 11.9264     57.3958
.00352  .00123  .00080  .00032  .00187  .00112  .00063  .00003  .00082  .00044  .00037
.00144  .00035  .00035  .00008  .00053  .00049  .00018  .00009  .00012  .00005  .00006
.00086  .00023  .00023  .00006  .00029  .00028  .00010  .00007  .00004  .00002  .00001
  -64.7   -52.0   -96.2   -55.2   -58.8  -151.4   -65.6  -138.1     8.4     5.2     2.1
   85.5   114.5    56.5   113.6    99.4    19.1    94.1   -10.4  -167.4  -170.0  -177.7
  109.5   147.0    92.7   148.8    50.5   -55.1    36.4  -170.4   -15.0     2.3     5.2
```

Loading tables for other sites can be obtained at:

http://froste.oso.chalmers.se/loading
OR http://geodac.fc.up.pt/loading/index.html

Loading Green's Function

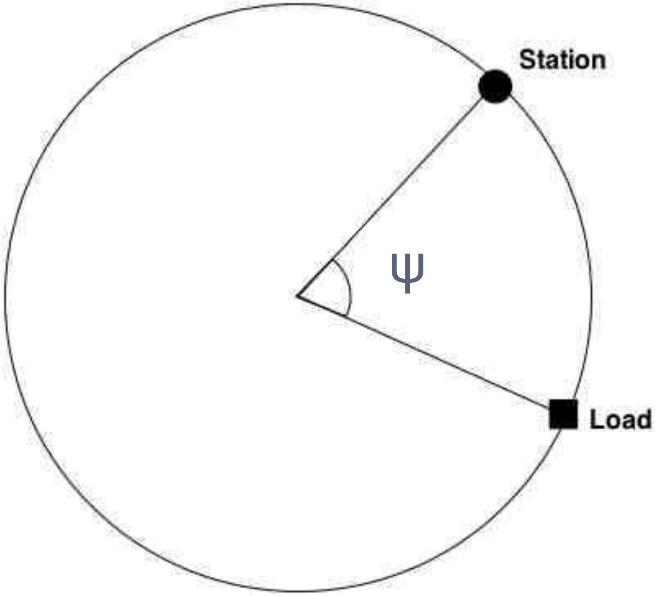

- Loading Green's function is the response at the station due to a mass load at an angular distance ψ from the station.
- Response is larger the closer the mass is to the station.
- Integration over the surface of the earth =>total adjustment of the station position caused by the surface mass distribution.
- Loading contribution is dominated by loading near the station as well as any large coherent regional loads far from the station.

Loading Green's Function

Expand the potential from point load (delta function at $\psi=0$)

$$\delta = \sum_{n=0}^{\infty} \Gamma_n P_n(\cos\psi) \quad => \quad \Gamma_n = \frac{2n+1}{4\pi a^2}$$

a = Earth radius

Load potential corresponding to point load distribution

$$V_2 = \sum_{n=0}^{\infty} \Phi_{2n} = 4\pi G a \sum_{n=0}^{\infty} \frac{\Gamma_n P_n(\cos\psi)}{2n+1}$$

$$\Phi_{2n} = \frac{4\pi G a}{2n+1}\Gamma_n = \frac{ag}{m_E}$$

Surface potential of the point mass load

Displacements (vertical and horizontal) and deformation potential arising from the potential [Farrell, 1972]:

$$\left.\begin{bmatrix} u_n \\ v_n \\ \phi_n \end{bmatrix} = \frac{\Phi_{2n}}{g} \begin{bmatrix} h_n \\ l_n \\ k_n \end{bmatrix} \quad \right\}$$

Love Numbers

Loading Green's Function

Expressions for the Green's functions (response to the point load)

Vertical displacement Green's function

$$G(\psi) = \frac{a}{m_E} \sum_{n=0}^{\infty} h_n P_n(\cos\psi)$$

Horizontal displacement Green's function

$$G(\psi) = \frac{a}{m_E} \sum_{n=0}^{\infty} l_n \frac{\partial P_n(\cos\psi)}{\partial \psi}$$

[See Farrell (1972) for tricks used to sum these series]

Loading Green's Function

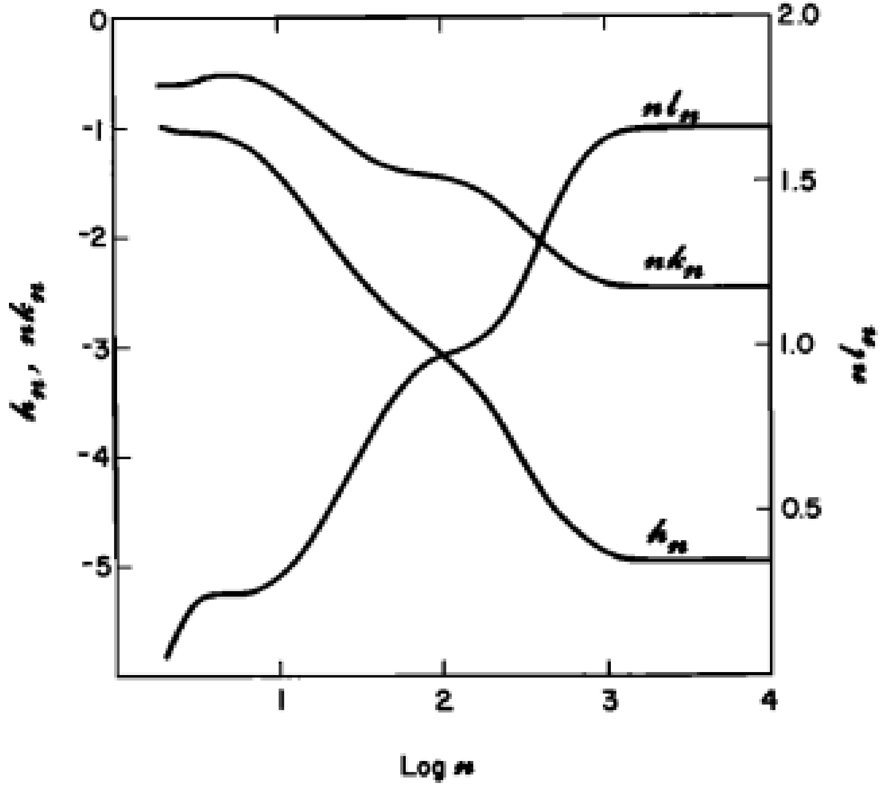

Fig. 1. Love numbers for a unit mass load on the surface of a Gutenberg-Bullen A earth model. Selected values are listed in Table A2. At $n = 10{,}000$, the computed Love numbers agree with the Boussinesq approximation to within 1%. The Love numbers for the other earth models differ significantly from these Love numbers above $n = 20$ to 30.

Loading Green's Function

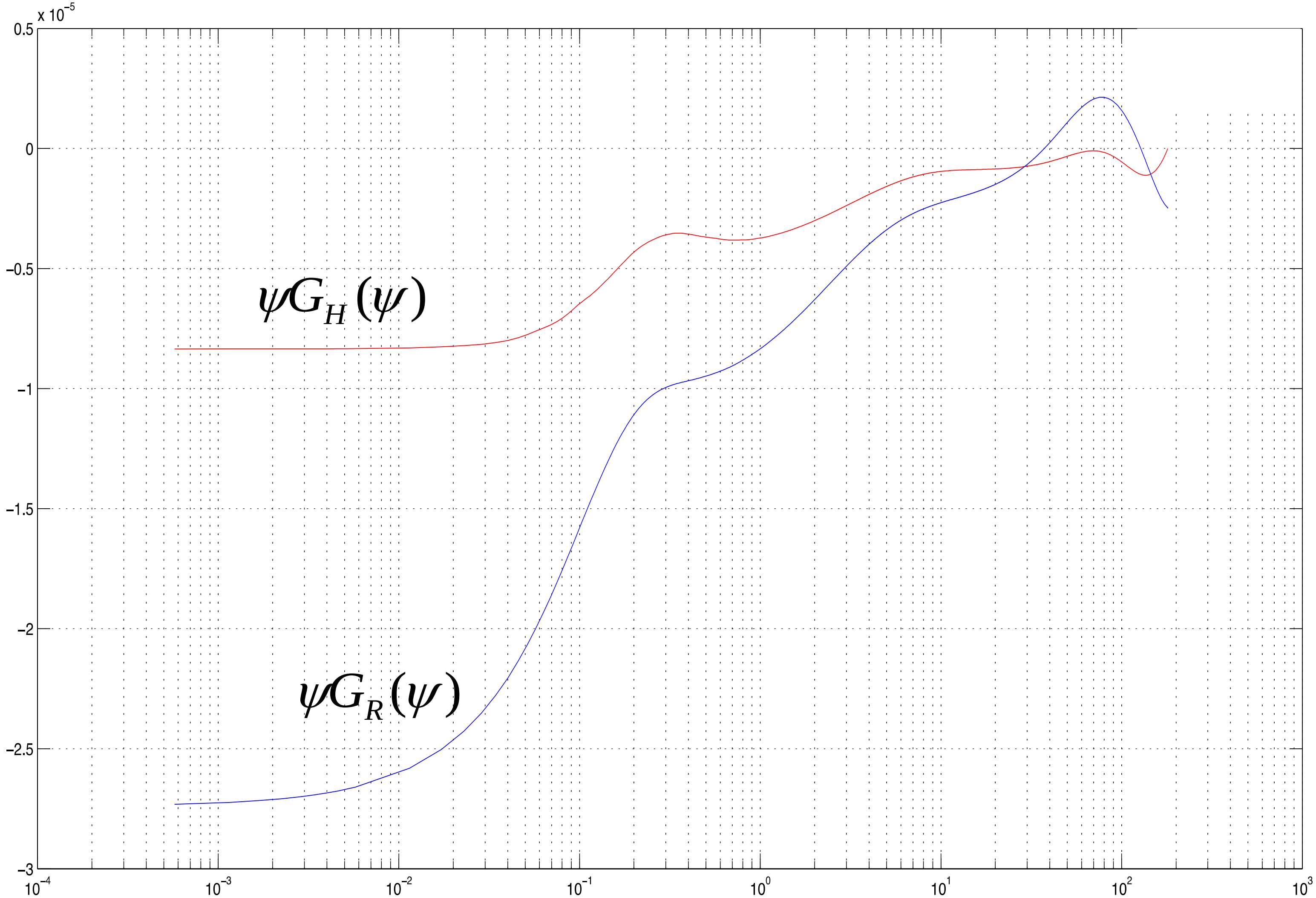

ψ (Angular separation of site and load)

Loading Green's Function

$$u_v(\lambda,\phi,t) = \iint \Delta m(\lambda',\varphi',t) G_R(\psi)\cos(\varphi')\, d\lambda'\, d\phi'$$

$$\begin{bmatrix} u_E(\lambda,\phi,t) \\ u_N(\lambda,\phi,t) \end{bmatrix} = \iint \begin{bmatrix} \sin(\alpha) \\ \cos(\alpha) \end{bmatrix} \Delta m(\lambda',\varphi',t) G_H(\psi)\cos(\varphi')\, d\lambda'\, d\phi'$$

α is the angle between the vector pointing from the site to the mass point and the site local reference direction (north)

- We need to set up an appropriate grid for integration
- The Green's function is singular => the grid must be increasingly finely divided the closer the mass points are to the site (as ψ -> 0) to account for the rapid increase in the Green's function.

Mass Loading

Why Investigate Mass Loading Effects?

Annual signals are clearly seen in observed VLBI baseline length and site position time series

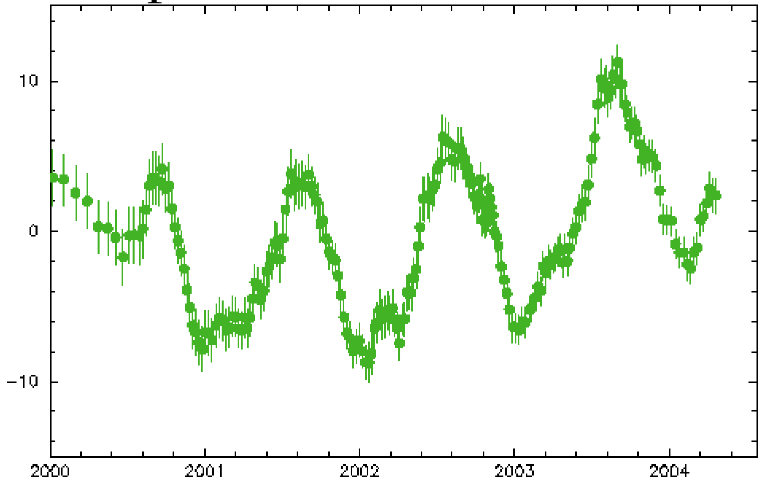

Baseline length time series (in mm) for Algonquin Park (Ontario) to Wettzell (Germany) smoothed with 2 month boxcar filter.

- Mass loading effects can produce site vertical variations of 15-20 mm and annual amplitudes as large as 4 mm at VLBI stations
- For problems like determining the rate of global sea level rise, expected to be ~1-2 mm/year, we need to monitor nontectonic VLBI site position rates at the sub millimeter level

Effect of Pressure Loading at Westford

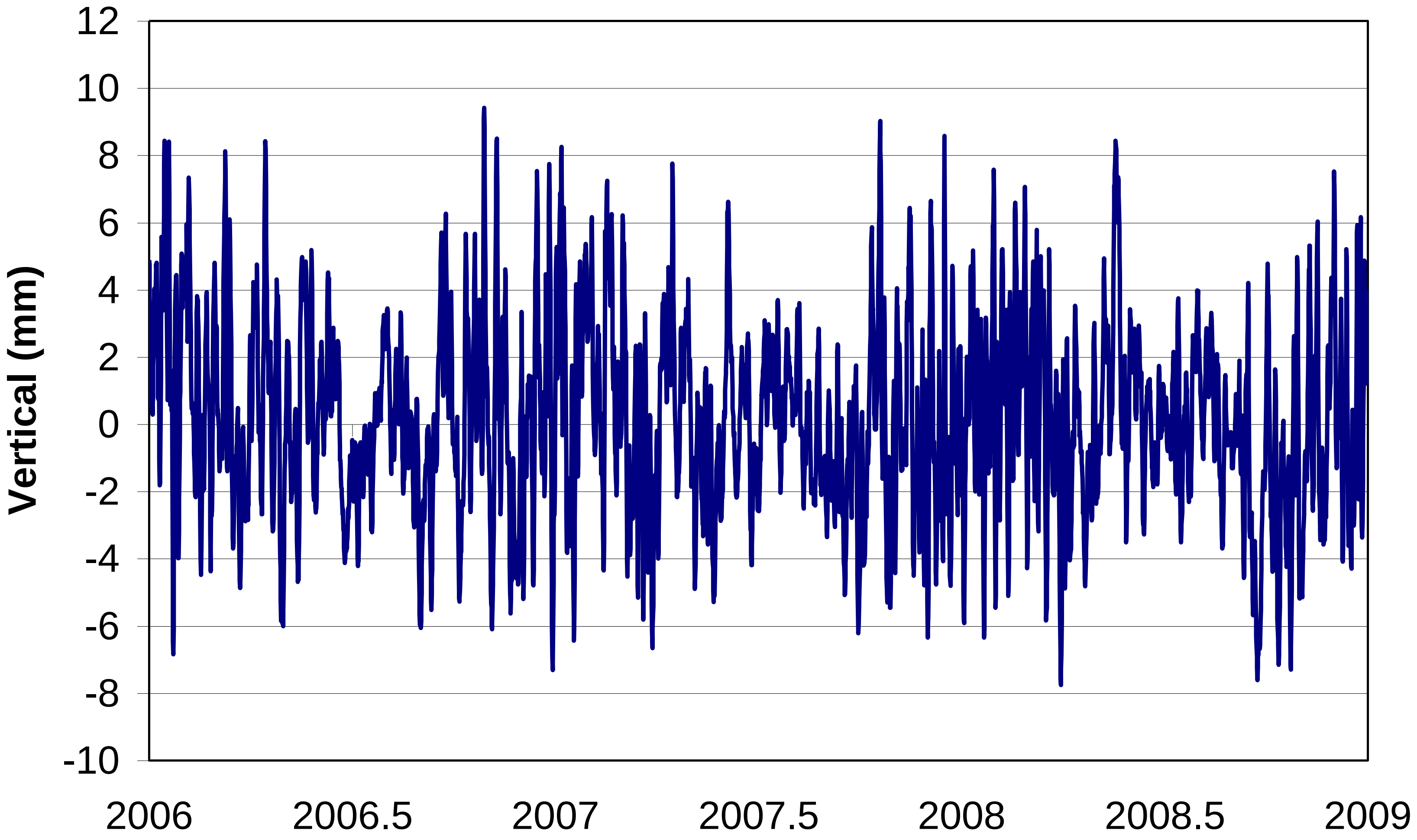

Pressure Loading Sensitivity ~ 0.2 – 0.6 mm/mbar

Effect of Pressure Loading at Westford

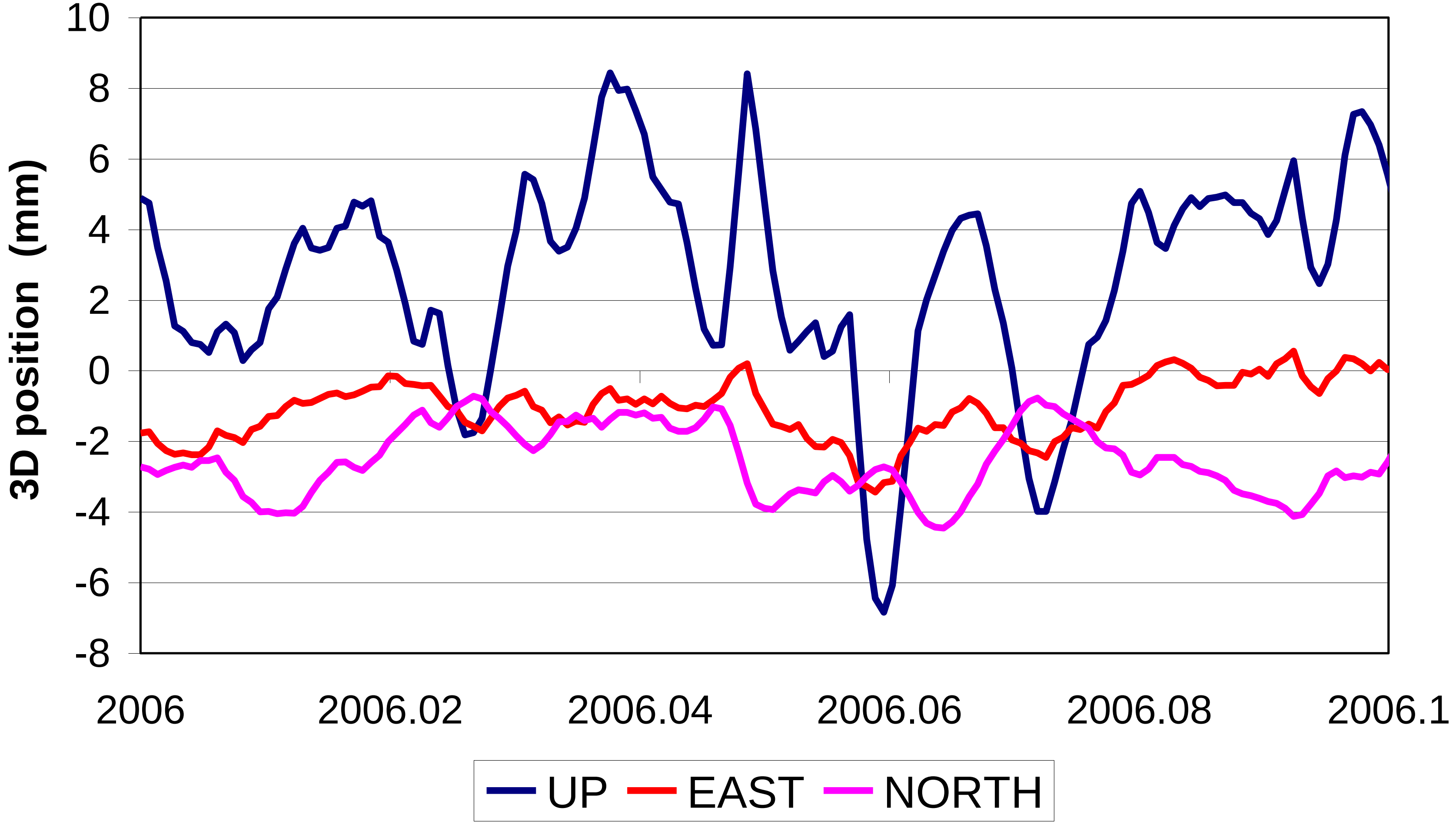

Atmospheric Pressure Loading

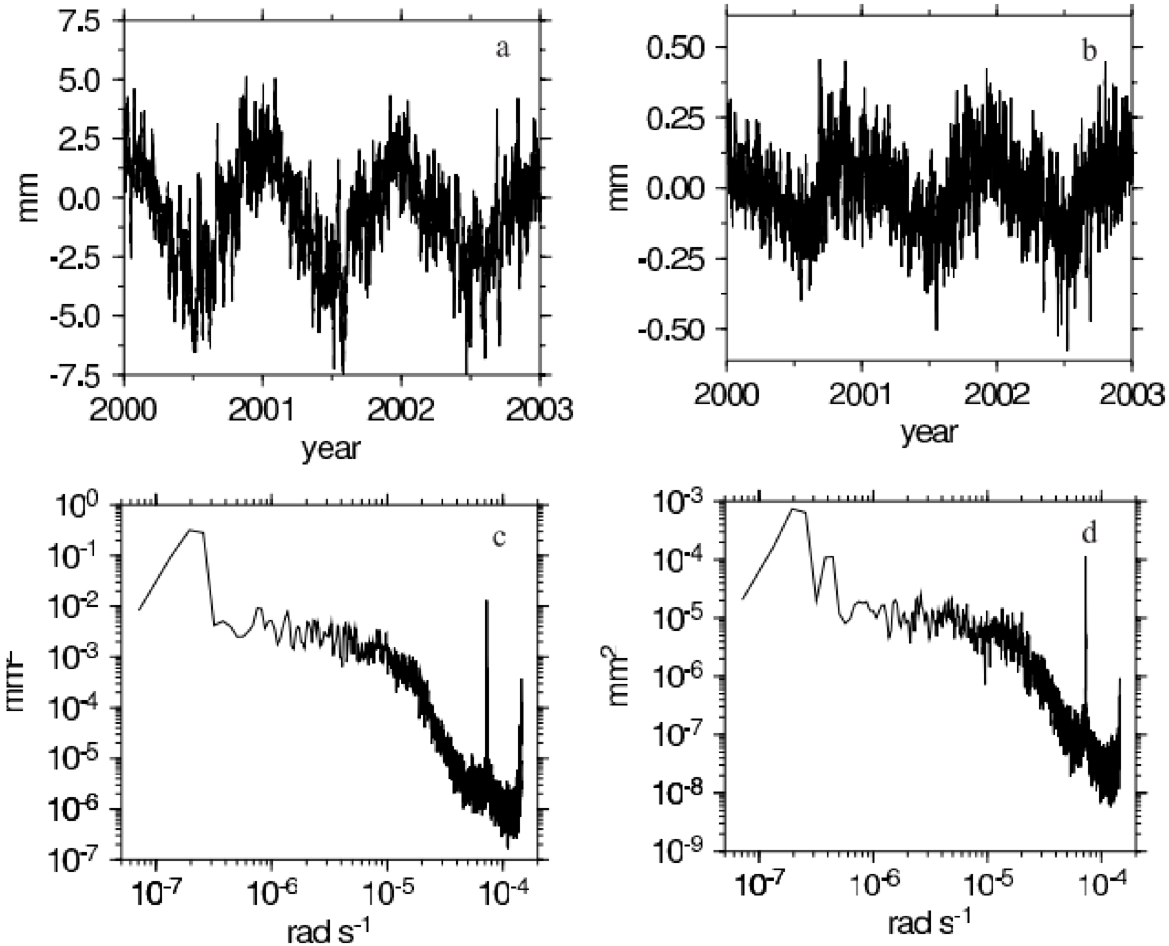

Figure 2. (a) Vertical and (b) east displacements induced by atmospheric pressure loading at the station Hartrao. Power spectrum of the (c) vertical and (d) east displacements.

- Low-latitude station
- strong wideband annual and semiannual signals
- relatively weak signal for periods below 10 days
- except strong S1 and S2 peaks

Hartebeestok, South Africa

Atmospheric Pressure Loading

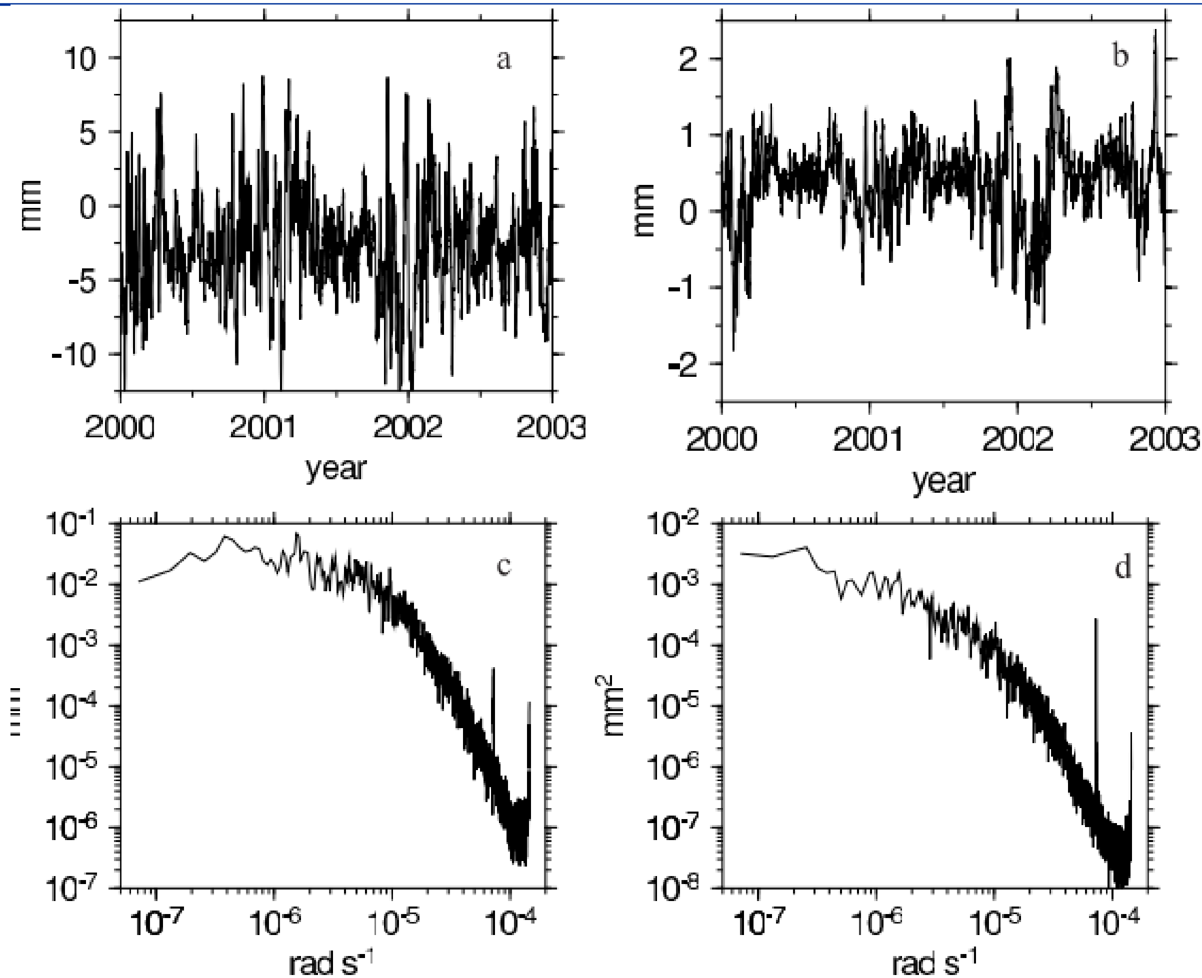

Figure 1. (a) Vertical and (b) north displacements induced by atmospheric pressure loading at the station Wettzell. Power spectrum of the (c) vertical and (d) north displacements.

Wettzell, Germany

- Midlatitude station
- S1 and S2 signal
- horizontal ~ 1/5 vertical variation

Atmospheric Pressure Loading

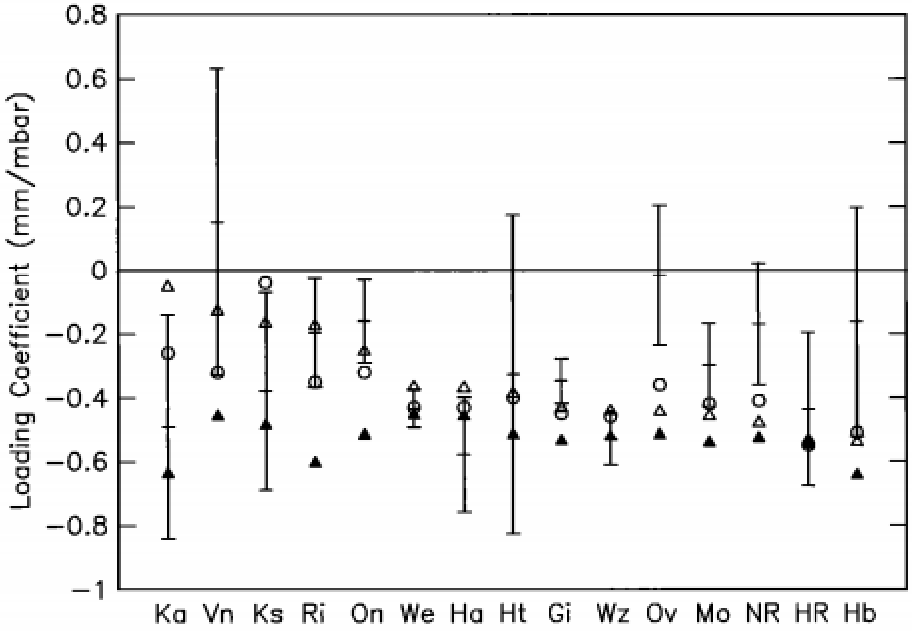

Figure 2. Pressure loading coefficients (mm/mbar) derived directly from VLBI data from 1979-1992 for stations that observed for 50 or more sessions. For comparison, the coefficients derived theoretically by *Manabe et al.* [1991] are shown for the inverted barometer (open triangles) and noninverted barometer (solid triangles) cases. In addition, the inverted barometer theoretical coefficients derived by *vanDam and Herring* [1994] are plotted (open circles). The stations are ordered by the inverted barometer values: KAUAI (Ka), VNDNBERG (Vn), KASHIMA (Ks), RICHMOND (Ri), ONSALA60 (On), WESTFORD (We), HAYSTACK (Ha), HATCREEK (Ht), GILCREEK (Gi), WETTZELL (Wz), OVRO 130 (Ov), MOJAVE12 (Mo), NRAO85 3 (NR), HRAS 085 (HR), and HARTRAO (Hb). The product of the rms pressure variation and the magnitude of the loading coefficient at each site is the expected rms vertical variation.

- Simple local loading model:

$$Up = \alpha_{pressure}(P - P_{ref})$$

- Pressure loading admittance, α estimated from VLBI data (mm/mbar)
- Estimated admittances closer to convolution model admittances, where inverted barometer was assumed

Hydrology Loading

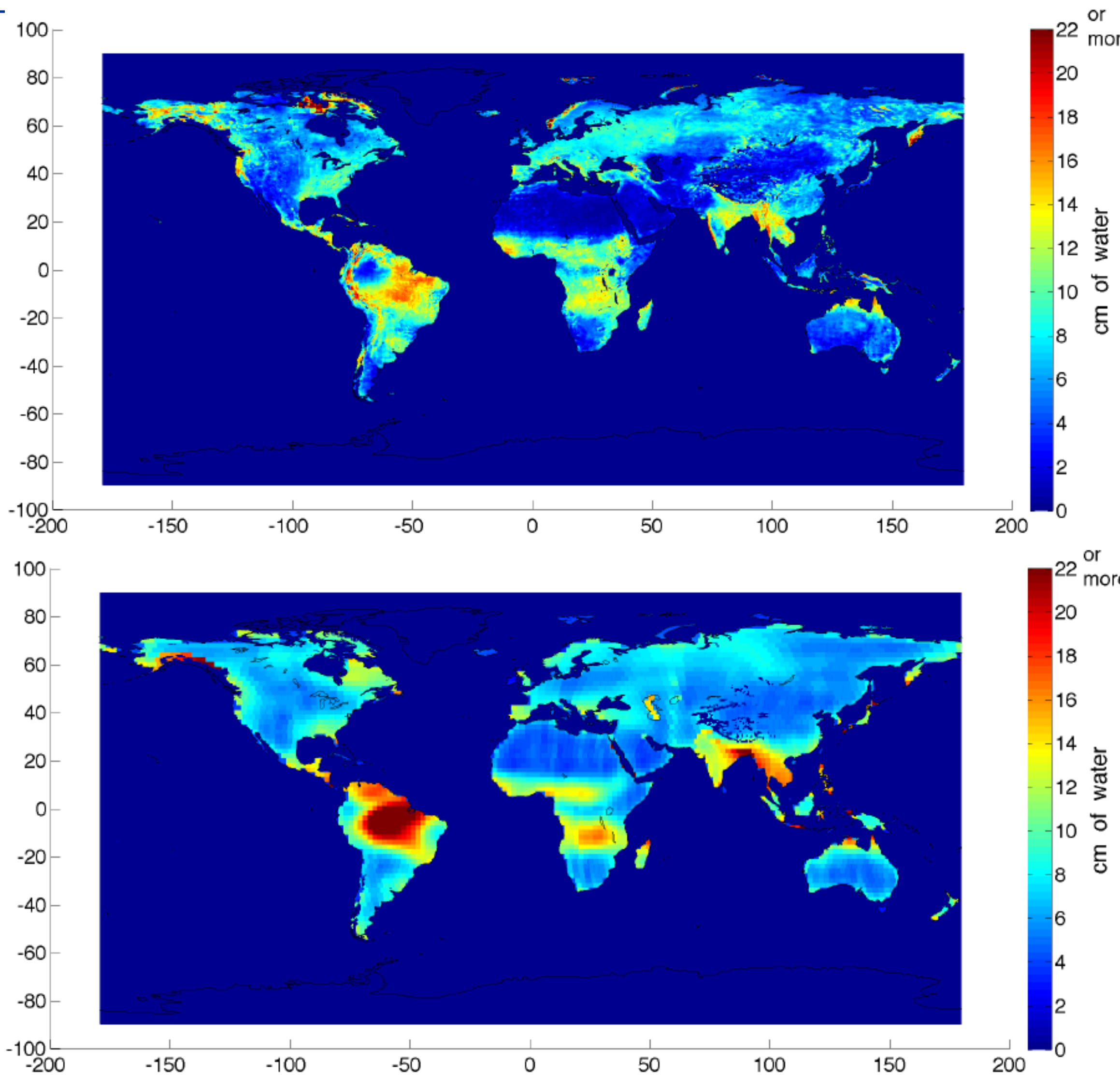

- NASA GLDAS hydrology model (Rodell et al. 2004)
- Contributions from soil moisture, snow water, plant canopy surface water storage

GRACE mass is in equivalent cm of water

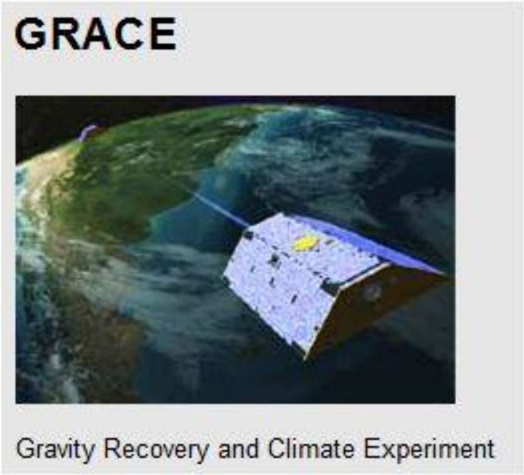

Hydrology Loading

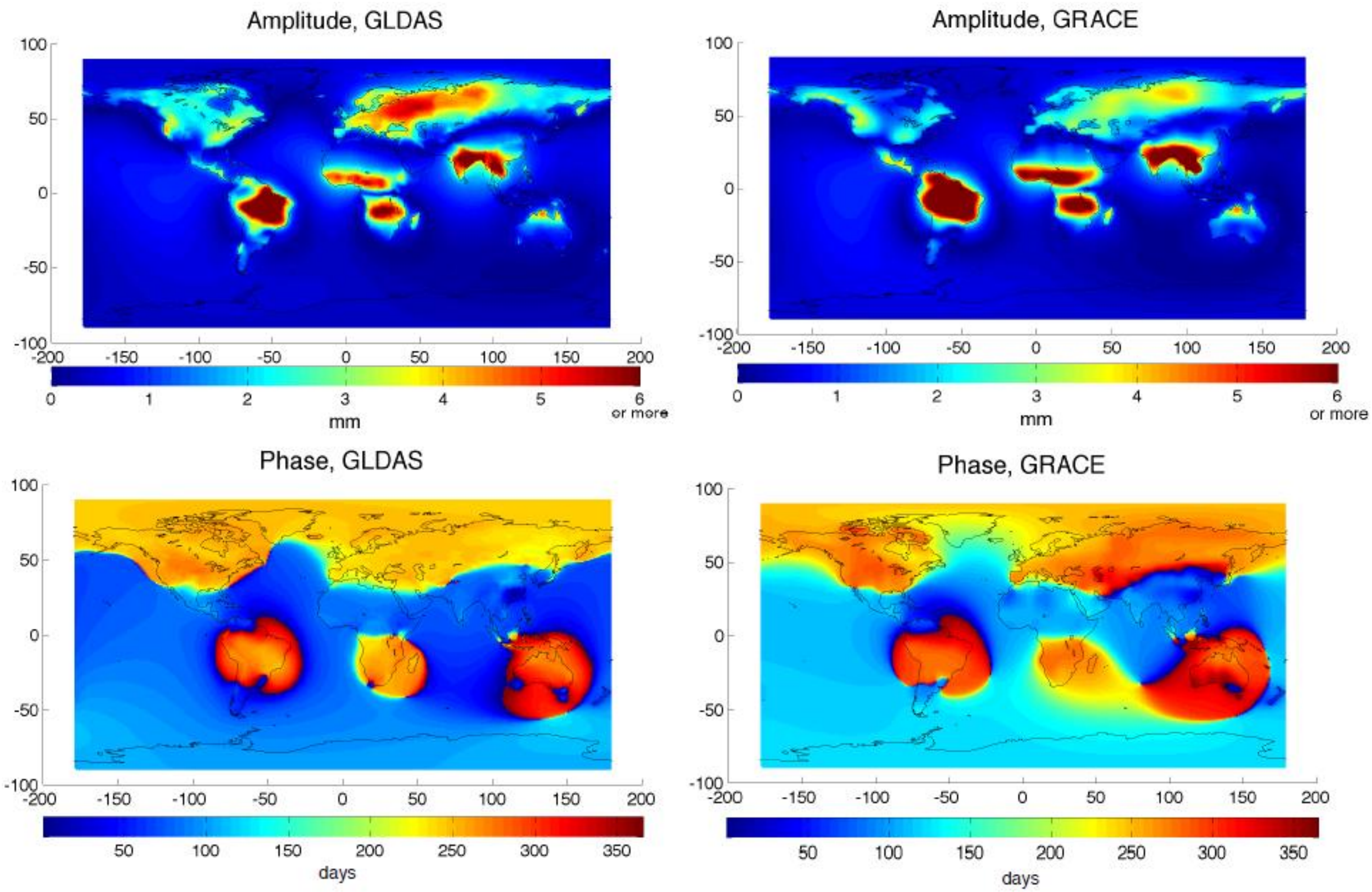

- Compute site loading convolving over hydrology mass distributions
- Annual amplitude shown above

Hydrology Loading

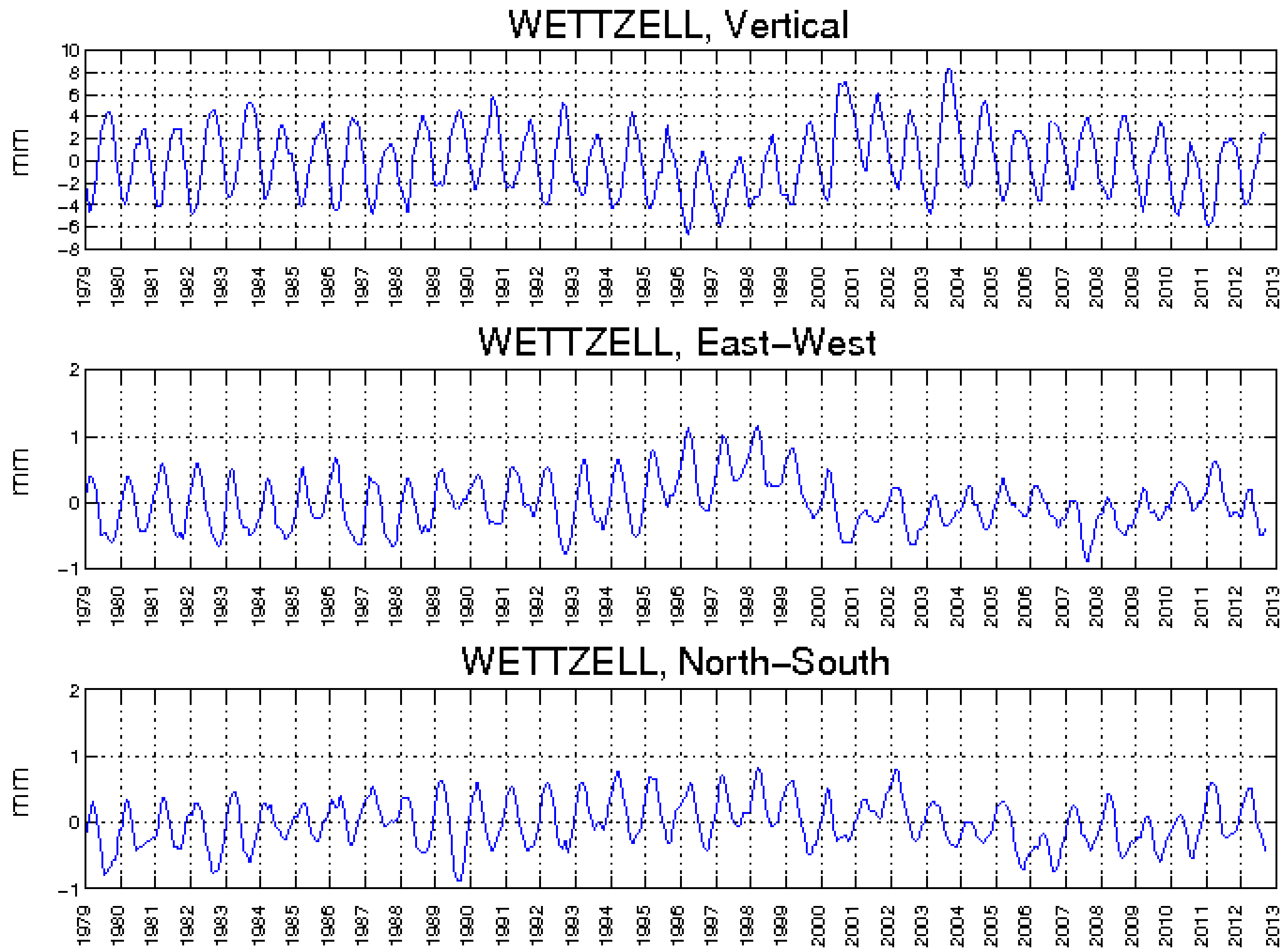

Hydrology Loading

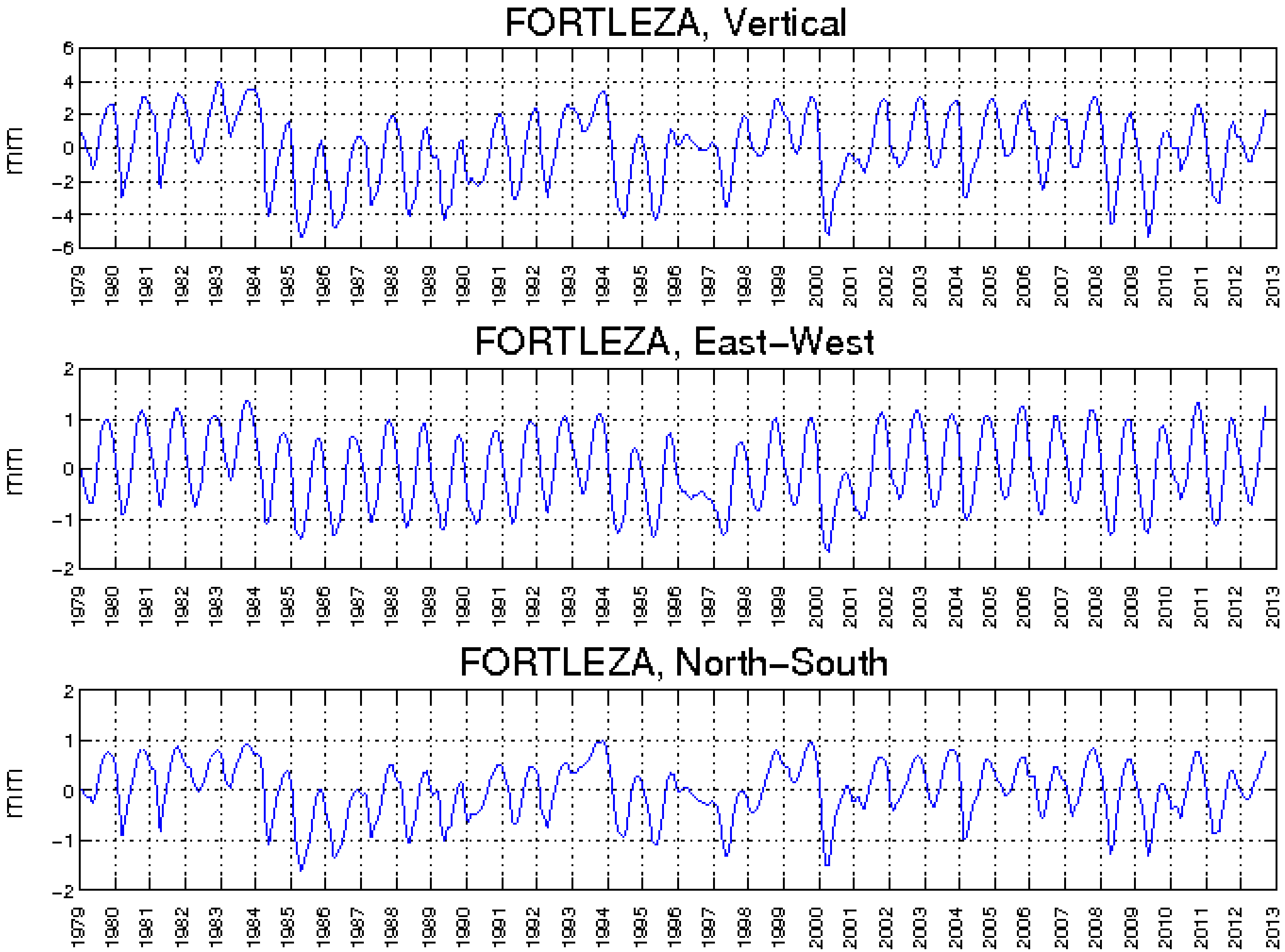

Hydrology Loading

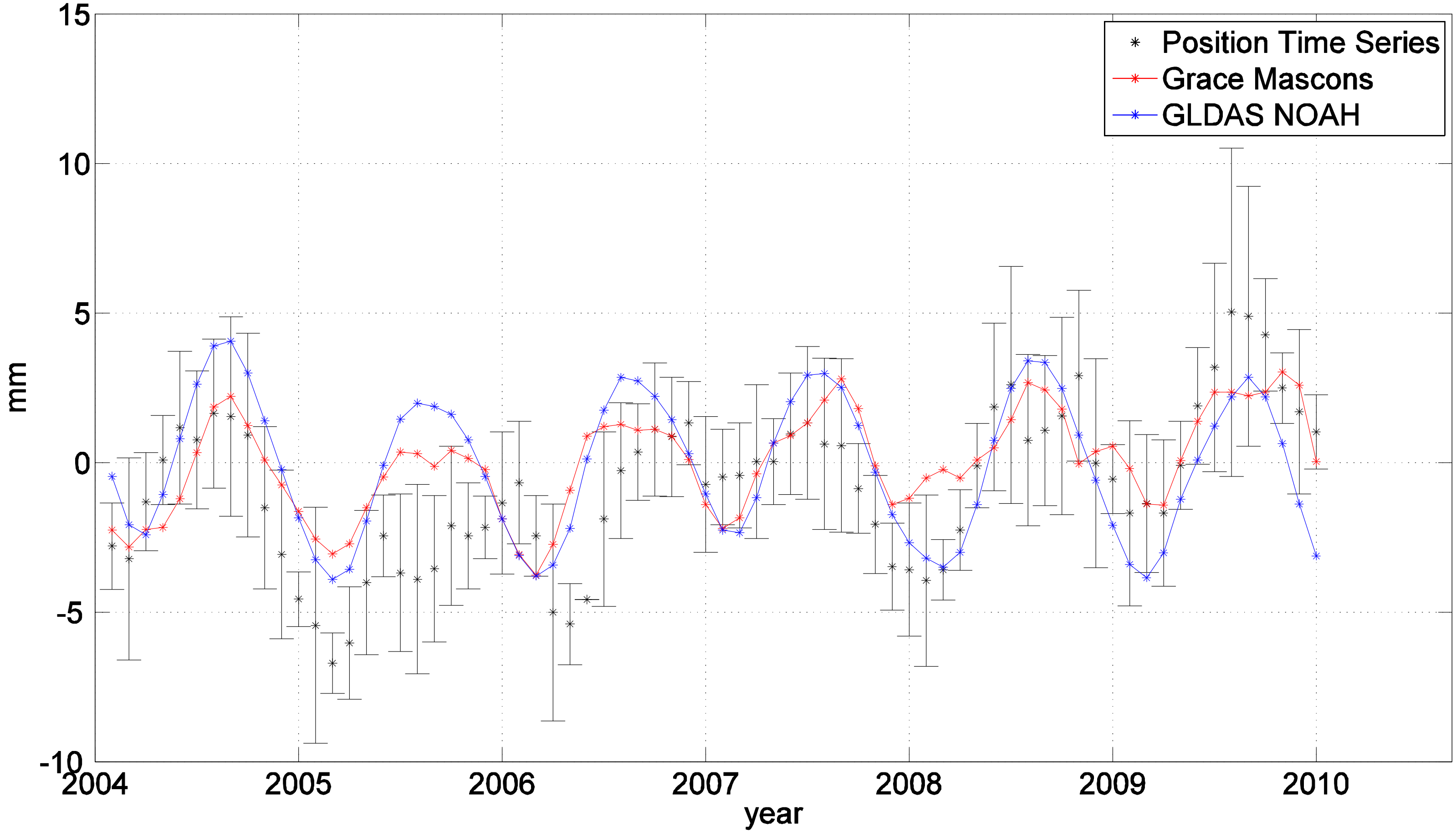

Position time series is a monthly averaged VLBI vertical series for Wettzell, Germany

Nontidal Ocean Loading

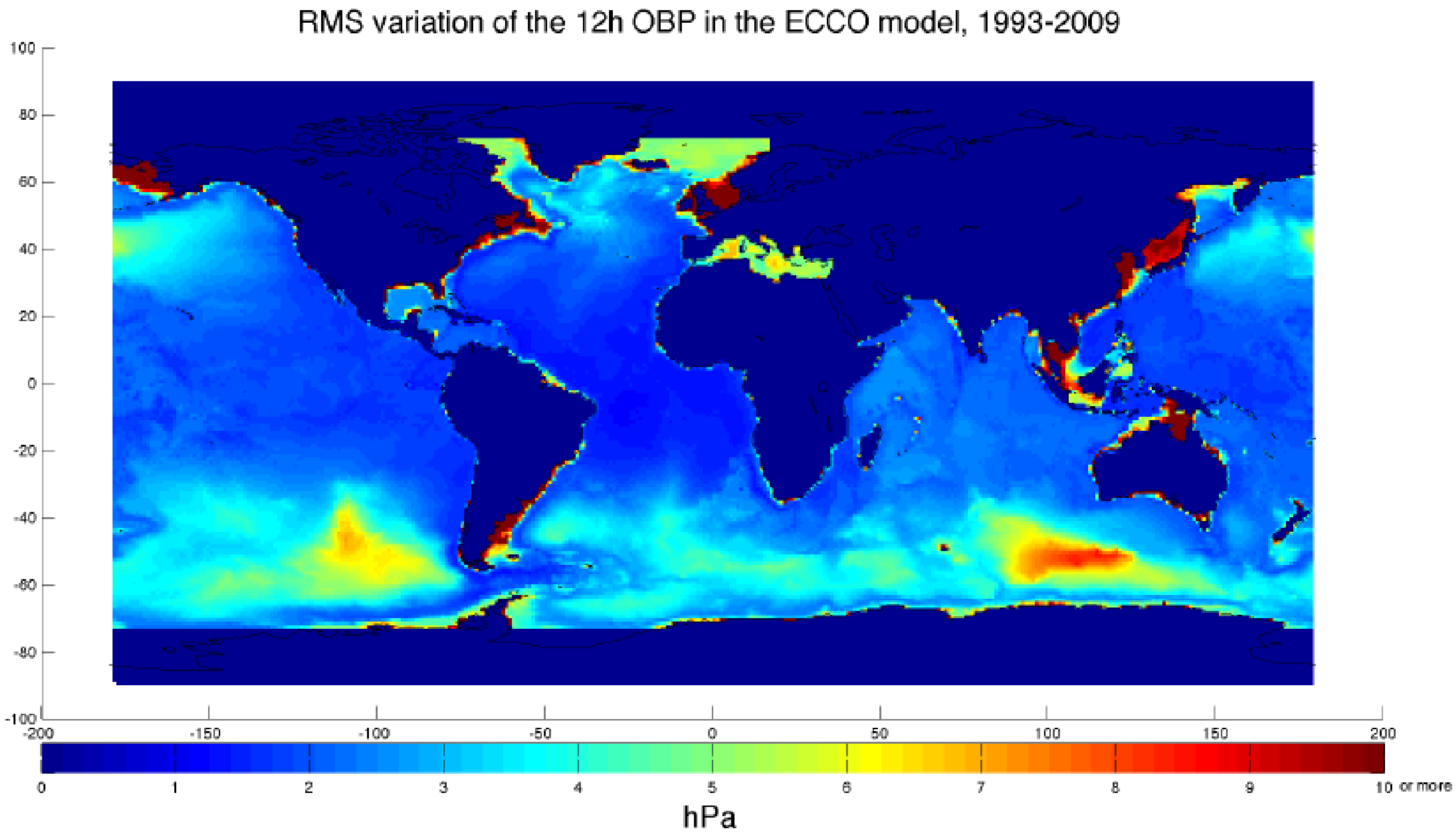

- JPL ECCO ocean model
- Used 12-hour ocean bottom pressure since 1993
- Oceanic volume (not mass) conserving
- Site displacement loading computed by usual Green's function approach

Nontidal Ocean Loading

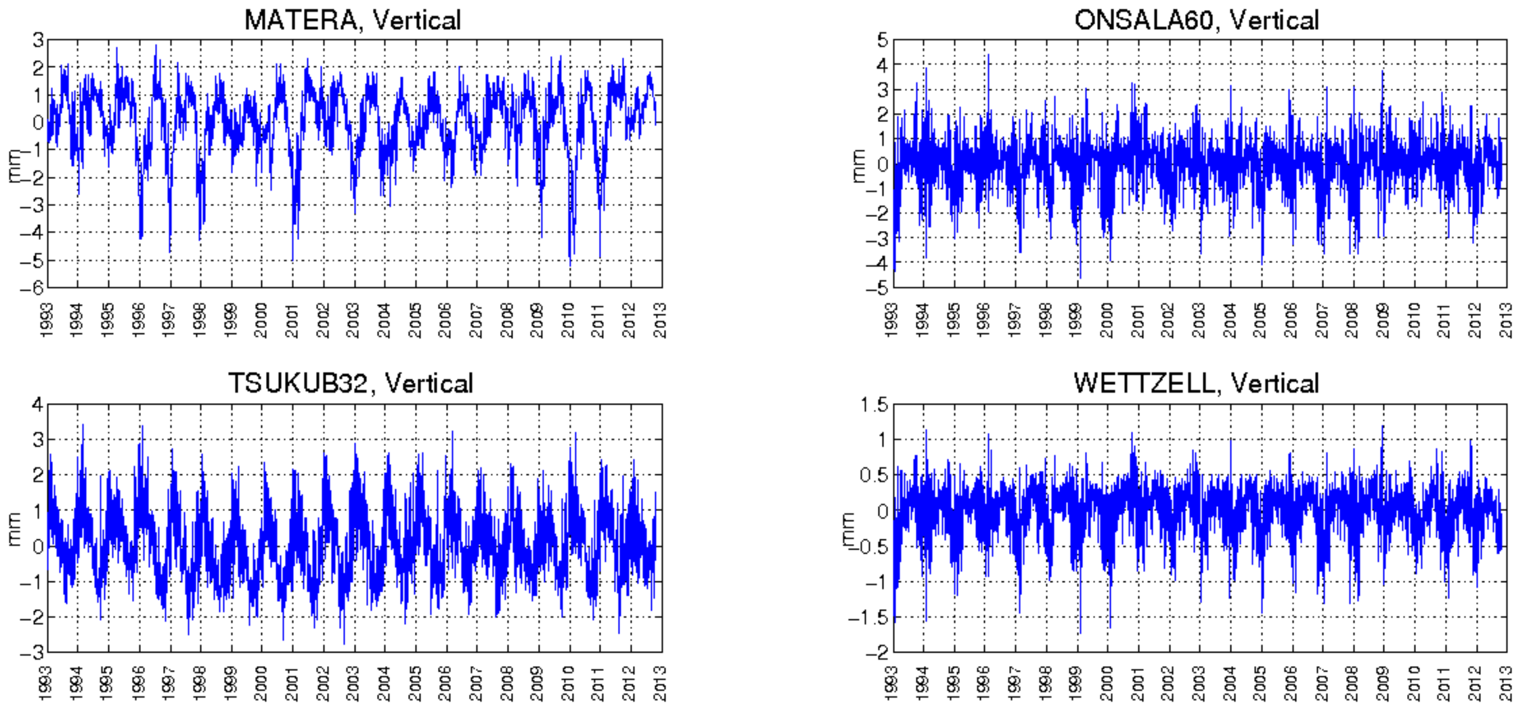

- Typical vertical loading series at VLBI sites:
  Coastal sites: Matera (Italy) rms 1.18 mm, Onsala (Sweden) rms 0.85 mm, Tsukuba(Japan) rms 0.89 mm
  Inland site: Wettzell (Germany) rms 0.31 mm
- RMS variation is much smaller than VLBI residual vertical RMS

Nontidal Loading Series

Hydrology Loading
- GLDAS NOAH model since 1979, updated when data is available
- Monthly series for 170 VLBI stations
- 1x1 degree gridded map with loading series for each lattice point
- http://lacerta.gsfc.nasa.gov/hydlo/

Nontidal Ocean Loading
- JPL ECCO model since 1993, updated when data is available
- 12-hour resolution series for 170 VLBI stations
- 1x1 degree gridded map will be generated in future
- http://lacerta.gsfc.nasa.gov/oclo/

Atmospheric Pressure Loading
- Maintain Petrov-Boy series
- NCEP Reanalysis since 1979, updated when data is available
- 6-hour series for 824 VLBI+GPS+SLR sites
- 2.5x2.5 degree gridded map with loading series for each lattice point
- http://lacerta.gsfc.nasa.gov/aplo_eph/

Antenna Thermal Deformation

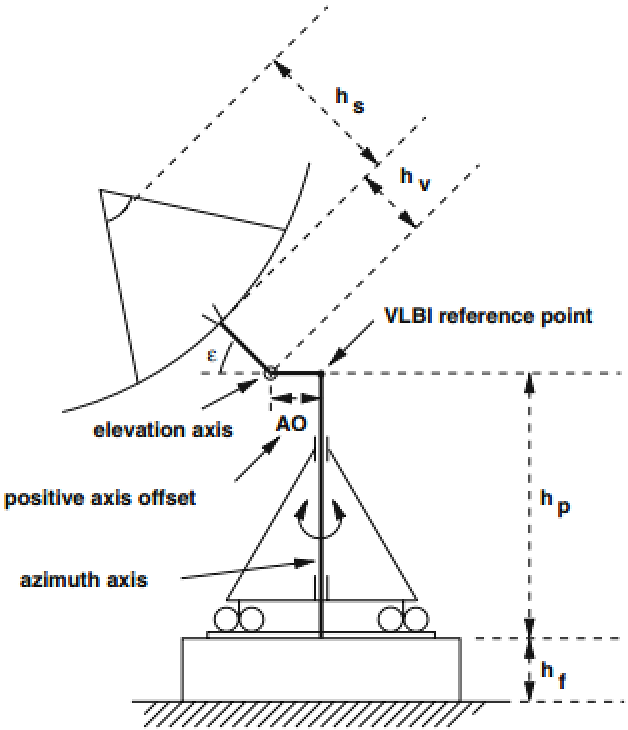

Fig. 1 Alt-azimuth telescope mount with positive axis offset

(a) For alt-azimuth mounts

$$\Delta\tau_{\mathrm{therm},i} = \frac{1}{c} \cdot \left[\gamma_{\mathrm{f}} \cdot (T(t-\Delta t_{\mathrm{f}}) - T_0) \cdot (h_{\mathrm{f}} \cdot \sin\varepsilon) + \gamma_{\mathrm{a}} \cdot (T(t-\Delta t_{\mathrm{a}}) - T_0) \cdot (h_{\mathrm{p}} \cdot \sin\varepsilon + AO \cdot \cos\varepsilon + h_{\mathrm{v}} - F_{\mathrm{a}} \cdot h_{\mathrm{s}})\right]. \qquad (2)$$

Expansion coefficients $\gamma \sim$ 1.0-1.2 x10-5/ºC

See A. Nothnagel (2009) for more on deformation model for all types of antenna mounts

Antenna Thermal Deformation

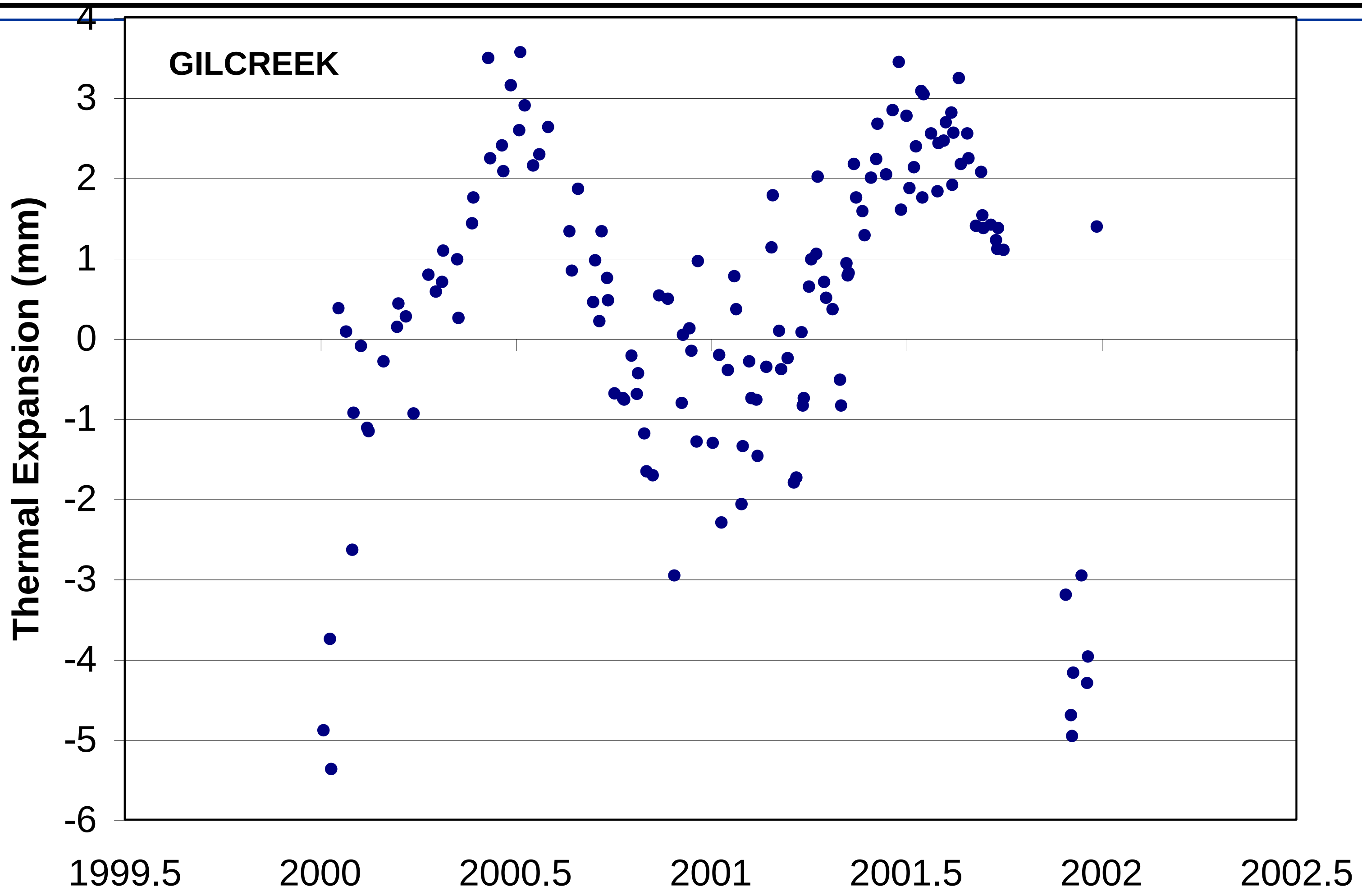

Fairbanks, Alaska antenna height ~ 15 m, annual temperature swing ~ 40 K, expansion coefficient ~ 1.2x10-5 => peak-to-peak variation ~ 7 mm

References

Farrell, W.E., Deformation of the earth by surface loads, Rev. Geophys. Space Phys., 10, 761-797, 1972.

Hartmann, T., and H.-G. Wenzel, The HW95 tidal potential catalogue, Geophys. Res. Lett., 22, no. 24, 3553-3556, 1995.

Petit, G. and B. Luzum (eds.) , IERS Conventions (2010), IERS Tech. Note 36, International Earth Rotation and Reference Systems Service, 2010.

Ray, R.D., A global ocean tide model from TOPEX/POSEIDON altimetry: GOT99.2, NASA/TM-1999-209478, NASA Goddard Space Flight Center.